Assessment of MDEA absorption process for sequential H_2S removal and CO_2 capture in air-blown IGCC plants

Stefania Moioli [a], Antonio Giuffrida [b,*], Matteo C. Romano [b], Laura A. Pellegrini [a], Giovanni Lozza [b]

[a] *Politecnico di Milano, Dipartimento di Chimica, Materiali e Ingegneria Chimica "G. Natta", Piazza Leonardo da Vinci 32, 20133 Milano, Italy*
[b] *Politecnico di Milano, Dipartimento di Energia, via Lambruschini 4, 20156 Milano, Italy*

This work deals with pre-combustion CO_2 capture by Methyldiethanolamine (MDEA) scrubbing in air-blown integrated gasification combined cycles (IGCCs). Two types of coal, with low- and high-sulphur content, are considered as fuel input in power plants, as well as two combustion turbines, with different turbine inlet temperature, representative of state-of-the-art and advanced technologies.

The gasification section and the power island are simulated by means of the proprietary code GS. Acid gas removal (AGR), consisting in the sequential H_2S removal and CO_2 capture from the syngas by MDEA solvent, is calculated with Aspen Plus®. MDEA concentration and solvent circulation are varied in each of the assessed cases to comply with the target CO_2 capture efficiency and with the CO_2 and H_2S purity spec-ifications. The resulting heat duties for H_2S and CO_2 stripping, the consumption of the auxiliaries in the AGR plants, as well as the CO_2 compression work are used to calculate the energy and mass balances of the integrated gasification combined cycles. Sensitivity analysis on the temperature approach in the recu-perative heat exchanger of the CO_2 capture section and on the pressure of the CO_2 stripping column have been performed to assess potential energy savings. Results are compared with benchmark IGCC plants without CO_2 capture.

Net electric efficiencies between 36.6% and 40.4%, with 95% of CO_2 capture efficiency, are achieved depending on the coal quality (i.e. the sulphur content), the combustion turbine technology and the MDEA regeneration pressure and heat exchanger temperature difference. Correspondingly, a specific primary energy consumption for CO_2 avoided (SPECCA) between 2.85 and 3.2 MJ=kg_{CO_2} for the low-sulphur coal cases and between 3.2 and 3.7 MJ=kg_{CO_2} for the high-sulphur coal cases have been calculated.

Highlights:
Air-blown IGCC plants with sequential H2S removal and CO2 capture are investigated.
Two MDEA-based processes are proposed for sequential H2S removal and CO2 capture.
The influence of a low- and a high-sulphur coal and of two combustion turbines is assessed.
Net efficiencies between 36.6% and 40.4%, with 95% of CO2 capture, are achieved.
Better IGCC performance is always achieved in case of low-sulphur coal gasification.

Keywords: Air-blown, CO2 capture, H2S removal, IGCC, MDEA

1. Introduction

The power sector of many emerging economies relies on coal-fired power plants which emit huge amounts of carbon dioxide (CO_2). For example, China currently generates up to 80% of its power by burning coal [1], while India obtains more than two thirds of its electricity from coal [2]. A promising technology to mitigate CO_2 emissions caused by coal-fired power plants is carbon capture and storage (CCS). In detail, CO_2 resulting from carbon oxidation is separated, compressed and transported to places where it can be stably stored, such as in underground geological formations. However, CCS systems require additional energy input, which reduces the efficiency of power plants [3,4]. The extent of this reduction depends on the applied technology, which in turn is influenced by the technology adopted for the conversion of the

Article history:
Received 24 April 2016
Received in revised form 12 August 2016
Accepted 26 August 2016
Available online 5 October 2016

* Corresponding author.
E-mail address: antonio.giuffrida@polimi.it (A. Giuffrida).

© 2016. This manuscript version is made available under the CC-BY-NC-ND 4.0 license http://creativecommons.org/licenses/by-nc-nd/4.0/Published Journal Article available at http://dx.doi.org/10.1016/j.apenergy.2016.08.155

Nomenclature

ADV	advanced
AGR	acid gas removal
BOP	balance of plant
CCS	carbon capture and storage
CT	combustion turbine
EBTF	European Benchmarking Task Force
HHV, LHV	higher, lower heating value, MJ/kg
HP, MP	high, medium pressure
HRSC	heat recovery steam cycle
HRSG	heat recovery steam generator
HT, LT	high, low temperature
IGCC	integrated gasification combined cycle
k	kinetic constant for reactions
K	equilibrium constant for reactions
L/G	liquid to gas ratio
$\dot{m}$	mass flow rate, kg/s
MDEA	Methyldiethanolamine
MHI	Mitsubishi Heavy Industries
NG	natural gas
NRTL	non-random two-liquid
p	pressure, bar
SCOT	Shell Claus off-gas treatment
SOA	state-of-the-art
SPECCA	specific primary energy consumption for CO_2 avoided, MJ/kg_{CO_2}
T	temperature, °C
TIT	turbine inlet temperature, °C
VLE	Vapor-Liquid Equilibrium
WGS	water-gas shift
x	mole fraction of component in the liquid phase
y	mole fraction of component in the vapor phase
η	efficiency

Subscripts

b	backward (related to chemical reaction)
el	electric
f	forward (related to chemical reaction)
j	equilibrium reaction
ref	reference
th	thermal

primary feedstock, which can be either combusted (as in coal-fired boilers) or gasified (as in IGCCs).

IGCC is a solution drawing the attention of the scientific community as a clean coal technology [5–15]. The current IGCC technology is mainly based on oxygen-blown gasification, but a significant activity on air-blown gasifiers has been conducting during the last recent years by Mitsubishi Heavy Industries in Japan, where the 250 MW_{el} demonstration IGCC plant in Nakoso was started up in 2007 [16,17]. Shifting from oxygen- to air-blown gasification technology implies the economic advantage related to the much smaller air separation unit and to the potentially higher cycle efficiency [18]. In perspective, IGCC efficiency values as high as 53% may be obtained based on advanced technologies such as 1500 °C-class combustion turbine and hot fuel gas clean-up [19].

Focusing on CCS solutions, IGCC technology is highly suitable for the integration of pre-combustion carbon capture systems [8]. However, despite a number of papers dealing with CO_2 capture in oxygen-blown IGCC plants have been published [20–25], literature is lacking of similar works on air-blown gasification. Here, starting from a preliminary activity of the authors [26], the performance of air-blown IGCC plants with pre-combustion CO_2 capture is presented and discussed. Although both physical and chemical absorption processes may be suitable (e.g. Selexol™ process), a MDEA-based process is considered in this work. This option is justified by the limited CO_2 partial pressure in the coal-derived syngas, due to the significant nitrogen content, resulting from the use of air as oxidant in the gasifier.

As regards both H_2S removal and CO_2 capture, particular attention in modeling and simulation is paid to the acid gas removal (AGR) unit. In order to assess the effects of lower and higher sulphur content on the operation of the AGR plant, two coals are used as fuel input to the gasification system. Two combustion turbine technologies for shorter and longer term applications are also considered for the topping cycle, resulting in four IGCC cases with CO_2 capture assessed and compared with the corresponding benchmark cases without CO_2 capture. The thorough analysis presented in this work aims at improving the understanding of the possible design and of the potential performance of pre-combustion CO_2 capture in air-blown IGCC plants, for which no detailed information is available in the current literature.

2. The IGCC plant with CO_2 capture

The IGCC plants considered in this work consist of one gasification train, producing syngas for one combustion turbine in combined cycle configuration. The plant configuration is schematized in Fig. 1, where coal (1) is loaded with a dry lock hopper system by means of a fraction of the CO_2 captured in the AGR plant (2). In this case, the small air separation unit [16,17] used in the power plant without CO_2 capture to produce the pure nitrogen for coal loading (see Fig. 2), is not necessary. By operating with CO_2 as gas for coal loading, gasification occurs in an atmosphere richer in CO_2 with respect to the common reference case with N_2 as coal loading gas. Although such a condition reduces the char conversion kinetics, the same operating temperature and fuel conversion of the reference case with N_2–based loading are maintained, in absence of specific information from manufacturers in the open literature, therefore assuming that proper adaptations to the gasifier geometry are made to achieve the target carbon conversion. The air-blown coal gasification system developed by MHI [16,17] is a water-wall, two-stage entrained flow gasifier. Such a configuration allows for a carbon conversion of the order of 99.9% in the bottoming combustion stage, where coal and recycled char are burnt at high temperature (about 1900 °C) with high air-to-coal ratio. In the topping stage, high-temperature syngas is chemically quenched and experiences a temperature drop of about 700 °C. Because of the lower temperature, the coal-derived gas exiting the gasifier contains a certain amount of unconverted carbon, which is separated and recycled back to the combustor stage. As shown in Fig. 1, the air for coal gasification (8) is extracted from the CT compressor outlet, partly cooled down to about 350 °C by producing HP steam and finally boosted to the gasification system. The coal-derived gas exiting the gasifier is cooled down to about 350 °C (11) by producing HP super-heated steam and is then further cooled down (12), before scrubbing, by economization of HP water. A sour WGS station, with two reactors and two heat

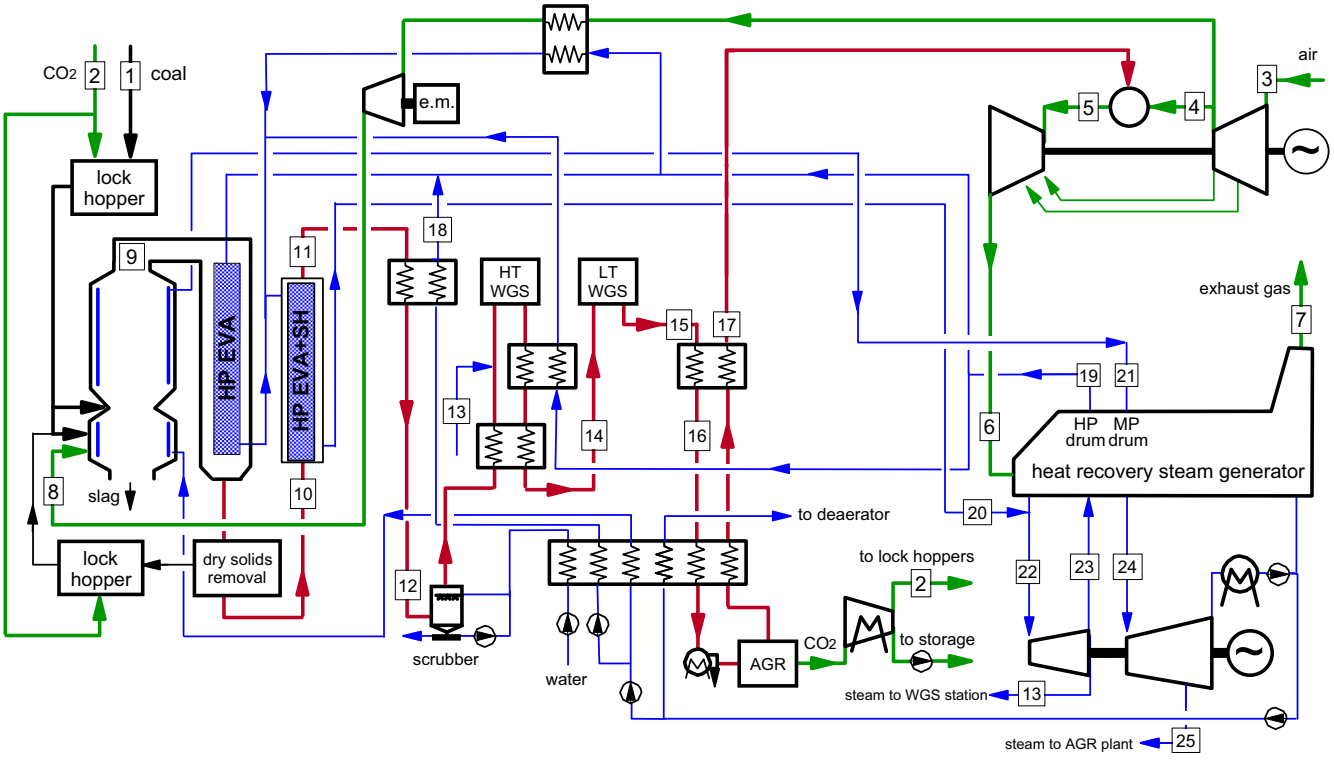

Fig. 1. Schematic layout of the IGCC plant with CO_2 capture.

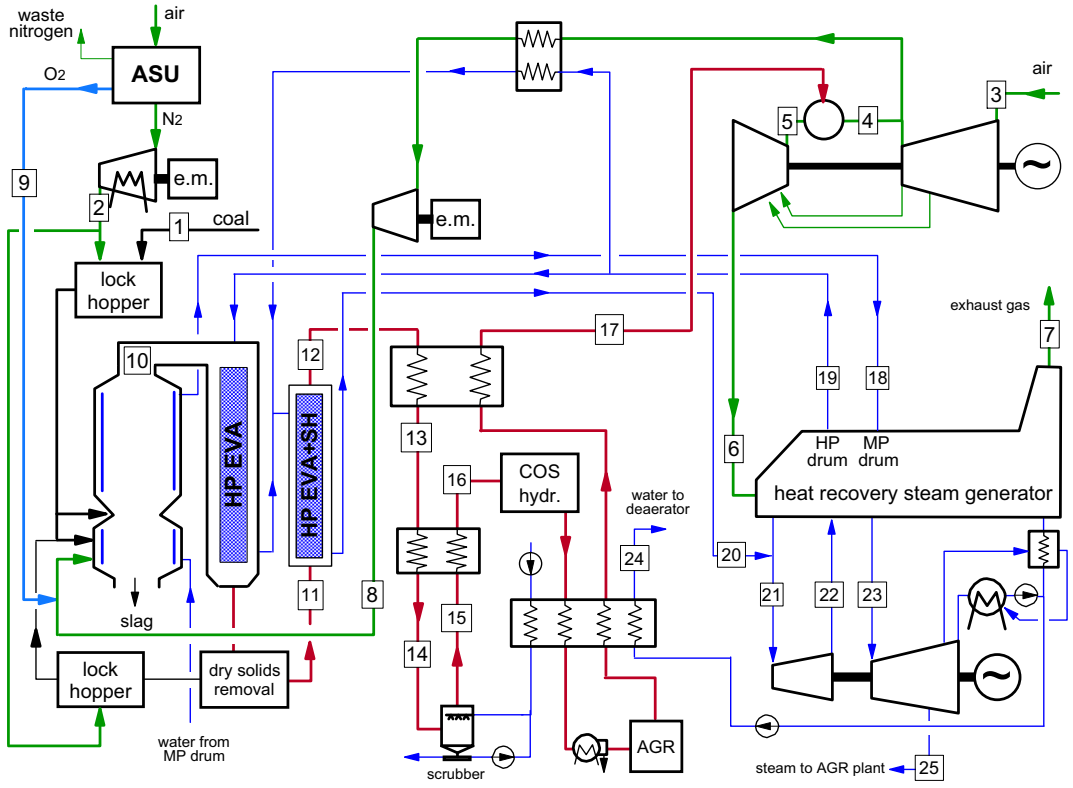

Fig. 2. Schematic layout of the IGCC plant without CO_2 capture.

exchangers, is present after the scrubber. In detail, the syngas exiting the scrubber is firstly pre-heated in a recuperative heat exchanger and then mixed with MP steam (13), extracted from the steam turbine, before entering the first WGS reactor. The shifted syngas exiting the HT-WGS reactor at temperature slightly lower than 500 °C is firstly cooled down to about 350 °C by producing HP

steam and by preheating the syngas exiting the scrubber. Then, the shifted syngas at about 210 °C (14) enters the LT-WGS reactor to complete the CO-to-CO_2 conversion. An overall CO conversion higher than 97% is obtained in the WGS station and more than 95% of the total carbon in the shifted syngas is finally present as CO_2. The shifted syngas exiting the LT-WGS reactor is cooled down to 150 °C (16) by heating the H_2-rich stream fuelling the combustion turbine. It is then further cooled down to near-ambient temperature for both H_2S removal and CO_2 capture, providing heat for pre-heating the clean syngas from the AGR plant and water for the steam cycle and for syngas scrubbing. The clean syngas exiting the AGR plant is heated up to about 230 °C (17) in recuperative heat exchangers before fuelling the combustion turbine, i.e. the topping cycle of the power station.

Two CT technologies have been considered in this work: a state-of-the-art (SOA) turbomachinery with TIT equal to 1305 °C and an advanced one with TIT equal to 1360 °C. Currently, SOA turbomachines using low heating value fuels such as synthetic gases are derived from natural gas (NG) machines and are operated with a maximum temperature lower than the design TIT employed with NG-fired turbines. In this work, the advanced machine is assumed to operate under syngas firing with the same TIT of 1360 °C of the original NG-fired turbine. For these cases, it is therefore assumed that market conditions and technological developments will allow operating a H_2-fired combustion turbine at the same TIT of current NG-fired turbomachinery. Besides, the two technologies differ in the fuel overpressure with respect to the air delivered by the CT compressor, as required at the fuel control valve (see Table 15). Thus, the CT technology also affects the operating pressure of the gasifier and the syngas cooling and treating stations, as well as the electric consumptions of the air booster, as better detailed hereafter. In detail, the gasification pressure for the plants with CO_2 capture resulted in 30.44 and 37 bar, depending on the CT technology and the related syngas overpressure at the fuel control valve. As regards the reference plants with no CO_2 capture, these pressures resulted in 28.06 and 34.12 bar. The higher pressure for the cases with CO_2 capture is due to the additional pressure drop through the water-gas shift process and through the supplementary heat exchangers. The CT exhaust heat is recovered in a two pressure level steam cycle with reheat, where the HP level is always fixed to 144 bar and the MP level is fixed to 40 or 36 bar, depending on the CT technology. The MP level is selected in order to match the pressure required at the WGS station, which depends on the gasifier pressure, since the steam for the water-gas shift process is assumed to be always extracted from the HP turbine outlet.

A detailed description of the benchmark IGCC plant without CO_2 capture, assumed as the reference case for performance comparisons, is omitted in this work. The configuration of the reference plant is shown in Fig. 2 and reproduces the one investigated by the authors in a previous work [18], with the addition of a heat exchanger before air boosting to the gasifier. In summary, the main differences with respect to the IGCC with CO_2 capture consist in: (i) a small ASU, which is used to produce nitrogen for the coal feeding and the char recycle systems and oxygen for enriching the oxidant air, (ii) no WGS reactors are employed, but a COS hydrolysis reactor is used to convert all the sulphur species into H_2S and to facilitate sulphur removal in the AGR unit, (iii) AGR is operated to remove only H_2S, as further discussed in the following sections.

The in-house code GS [27] has been used for the calculation of the plant mass and energy balances, with the exception of the AGR unit. The use of GS is mainly justified by the capability of reliably calculating cooled gas turbines by a built-in model, based on a stage-by-stage calculation approach which takes into account the blade cooling needs when firing H_2-rich fuels [28–30], and has been successfully used in past works to calculate a variety of IGCC plant configurations [31–37].

Tables A1–A3 in the Appendix detail the main assumptions for calculations of the two combustion turbines, of the gasification island and of the heat recovery steam cycle. They revise and integrate the ones reported elsewhere [7,18].

Throughout this work, the two coals reported in Table 1 have been considered as primary feedstock to the gasification system, in order to assess the effects of lower and higher sulphur content on the operation of the AGR plant. In detail, the cases investigated and discussed in the following are identified by a sequence of letters, where:

- C or N are used for cases with or without CO_2 capture, respectively,
- D or I are used for cases with Douglas Premium or Illinois #6 coal, respectively,
- SOA or ADV are used for cases with the state-of-the-art or the advanced combustion turbine, respectively.

3. The acid gas removal plant

The gas to be treated in the AGR plant contains both CO_2 and H_2S, two acid gases whose amount must be reduced before syngas combustion. Table 2 reports the main characteristics of the streams entering the AGR plant, according to the different analyzed cases.

Dealing with pre-combustion carbon capture, most of the CO_2 contained in the syngas must be removed before fuelling the combustion turbine. As anticipated, CO_2 capture is realized by chemical scrubbing in an absorber column. Afterwards, the CO_2-rich solution exiting the absorber is regenerated and the recovered CO_2 is sent to permanent storage after compression.

According to the EBTF guidelines [38], the CO_2 stream to storage should contain at most 200 ppm(v) of H_2S. In the syngas streams of the cases with CO_2 capture reported in Table 2, the amount of CO_2 is much higher than the one of H_2S. However, the content of H_2S is not low enough to make the CO_2 stream contain less than 200 ppm (v) of H_2S if co-absorption of both the acid gases is performed in a single column. Thus, H_2S and CO_2 must be sequentially removed in separate absorbers. Another important specification for the AGR plant is related to the H_2S content in the gas released by the H_2S stripper and fed to the Claus unit for sulphur recovery. A low H_2S content (below about 15%) in the feed of the sulphur recovery unit may require oxygen enrichment of the air used in the thermal stage or an oxygen-blown Claus to achieve sufficient furnace temperature. Due to the absence of the ASU in the IGCC with CO_2 capture, that may provide the required oxygen at relatively low additional cost, a minimum H_2S content of 20% in the sulphur recovery unit feed has been assumed, allowing a high sulphur recovery efficiency of 94–96% with a conventional three-stage Claus, with no need of pure oxygen production [40].

Selective absorption of H_2S in the presence of CO_2, especially in cases where the CO_2-to-H_2S ratio is very high, is accomplished by

Table 1
Composition (wt.%) and heating values (MJ/kg) of the two coals considered in this work.

	Douglas premium [38]	Illinois #6 [39]
C	66.52	61.27
H	3.78	4.69
O	5.46	8.83
N	1.56	1.10
S	0.52	3.41
Moisture	8.00	12.00
Ash	14.15	8.70
HHV	26.23	26.14
LHV	25.17	24.83

Table 2
Characteristics of the streams entering the AGR plant for all the considered cases.

	C-D-SOA	C-D-ADV	C-I-SOA	C-I-ADV	N-D-SOA	N-D-ADV	N-I- SOA	N-I-ADV
Pressure, bar	29.32	24.11	29.32	24.11	29.32	24.11	29.32	24.11
Temperature, °C				35				
Mass flow rate, kg/s	232.86	261.48	218.61	245.22	158.31	176.54	149.4	166.46
Component, mol%								
H_2S	0.07	0.07	0.49	0.49	0.09	0.09	0.64	0.64
CO_2	25.23	25.13	25.05	24.96	3.10	3.32	3.64	3.82
H_2O	0.19	0.23	0.19	0.23	0.19	0.23	0.19	0.23
CH_4	0.42	0.41	0.45	0.44	0.55	0.54	0.59	0.58
CO	0.78	0.74	0.82	0.79	27.77	27.36	26.60	26.24
H_2	27.84	27.25	29.08	28.50	9.86	9.63	12.60	12.34
N_2	44.95	45.63	43.40	44.06	57.78	58.17	55.11	55.51
Ar	0.53	0.54	0.52	0.52	0.66	0.67	0.63	0.64

means of an aqueous solution containing Methyldiethanolamine (MDEA), under proper operating conditions involving short contact times, exploiting in this way the much faster reaction kinetics of MDEA with H_2S with respect to CO_2. Because of its low vapor pressure, MDEA can be used in high concentrations without appreciable evaporation losses. Furthermore, it is highly resistant to thermal and chemical degradation and the heats of reaction with H_2S and CO_2 are low, allowing for limited heat duties for solvent regeneration with respect to alternative chemical solvents [41].

3.1. Amine scrubbing modeling

The amine scrubbing process is widely used in industry, but the design of the absorber is still difficult, due to the different phenomena involved: the mass transfer of CO_2 and H_2S is promoted by chemical reactions in the liquid phase, which influence the solubility of the acid gases. They diffuse from the bulk of the gas phase to the gas-liquid interface, which is governed by vapor-liquid equilibrium. In the liquid phase, diffusion from the gas-liquid interface to the bulk and simultaneous reactions with other species occur. The chemical reactions generate a gradient of concentrations of reaction products, which diffuse to the bulk of the liquid phase. Depending on the species involved, reactions can be kinetic-controlled or can attain chemical equilibrium. In both cases, operating conditions highly influence the extent of the reaction and the concentration of products. Therefore, thermodynamics, kinetics and mass transfer should be properly described, in order to avoid inaccurate representations of the process.

3.1.1. Thermodynamics

The absorption of acid gases in the amine solution involves the presence of chemical reactions occurring in the liquid phase:

$$2H_2O \overset{K_{H_2O}}{\rightleftarrows} H_3O^+ + OH^- \tag{1}$$

$$CO_2 + 2H_2O \overset{K_{CO_2}}{\rightleftarrows} HCO_3^- + H_3O^+ \tag{2}$$

$$H_2O + HCO_3^- \overset{K_{HCO_3^-}}{\rightleftarrows} CO_3^{2-} + H_3O^+ \tag{3}$$

$$MDEAH^+ + H_2O \overset{K_{MDEAH^+}}{\rightleftarrows} MDEA + H_3O^+ \tag{4}$$

$$H_2S + H_2O \overset{K_{H_2S}}{\rightleftarrows} H_3O^+ + HS^- \tag{5}$$

$$HS^- + H_2O \overset{K_{HS^-}}{\rightleftarrows} H_3O^+ + S^{2-} \tag{6}$$

Acid gases and amines react in water, producing a mixture composed of molecular and ionic species. The formers undergo also to Vapor-Liquid Equilibrium (VLE), while the latters are not present in the vapor phase, so complicating the description of the system.

The chemical equilibrium constants are computed according to Eq. (7).

$$\ln K_j = A_j + \frac{B_j}{T} + C_j \ln T + D_j T \tag{7}$$

The Electrolyte-NRTL model, developed by Chen and coworkers [42–45], has been used in this work, with proper parameters previously obtained by regression [46,47] and validation on experimental VLE data [48,49].

The model is an extension of the NRTL method proposed by Renon and Prausnitz [50]. It considers three types of cells and is based on two fundamental assumptions: the local electroneutrality and the like-ion repulsion. Each cell is composed of one species, surrounded by couples of anions and cations and molecules or by ions of the opposite charge and molecules, depending on the type of species at the center (molecule or ion, respectively). The number of different species involved and interacting each other is high [51]. However, the use of binary interaction parameters, properly chosen and determined [48,49], can allow a reliable representation of the VLE of the system.

3.1.2. Mass transfer

The chemical reaction of the solute with a component in the liquid phase has the effect of increasing the liquid film mass transfer coefficient, which results higher than the one obtained in the physical absorption process. An enhancement of the absorption phenomenon is observed, though its amount strongly depends on the rate of reactions. With very slow reactions, the dissolved molecules migrate to the bulk of the liquid before reactions occur, so the overall absorption rate is not appreciably increased by the occurrence of the chemical reaction. If very rapid reactions occur, on the contrary, the dissolved molecule suddenly undergoes chemical reactions, before reaching the bulk of the liquid phase (instantaneous regime) [52].

In the system involving reactions among acid gases, MDEA and water, the reactions involving CO_2 are quite fast at the typical operating conditions, but do not attain chemical equilibrium, while the reactions involving H_2S do. Thus, the phenomenon of diffusion with reaction needs to be modeled by considering also kinetically controlled reactions for CO_2:

$$CO_2 + OH^- \overset{k_{1f}}{\rightarrow} HCO_3^- \tag{8}$$

$$HCO_3^- \overset{k_{1b}}{\rightarrow} CO_2 + OH^- \tag{9}$$

$$CO_2 + MDEA + H_2O \overset{k_{2f}}{\rightarrow} HCO_3^- + MDEAH^+ \quad (10)$$

$$HCO_3^- + MDEAH^+ \overset{k_{2b}}{\rightarrow} CO_2 + MDEA + H_2O \quad (11)$$

Parameters of the kinetic constants, calculated according to the Arrhenius expression, can be found in literature [53,54].

Simulations of the scrubbing units have been performed by using the commercial software ASPEN Plus®, with the "rate-based" approach. The simulator is provided also with the "equilibrium based stage efficiency" approach, which can be a possible alternative to the CPU consuming "rate-based" calculation. However, it does not take into account the real mass and heat transfer phenomena that occur on a real tray or actual packing height [55,56]. Moreover, the stage efficiency cannot be kept constant along the column because of the presence of chemical reactions.

A deep insight into the mass transfer phenomenon has shown some inaccuracies of the film theory [57], by default implemented in the simulator for describing the mass transfer coefficient, when applied to amine scrubbing processes. As a matter of fact, the film theory considers a simple representation of mass transfer occurring across a stagnant film of given thickness [58–64]. The "rate-based" column has been coupled to a previously developed method based on the Eddy Diffusivity theory [65] and on the Interfacial Pseudo First Order assumption [66–68]. It is able to give the correct (square root) dependence on the diffusivity of CO_2 for the mass transfer coefficient. As a consequence, the CO_2 molar fraction profile along the column and the amount of absorbed CO_2 are predicted with appreciable accuracy [54], as reported elsewhere by comparison with experimental data of a pilot plant [69] and of an industrial plant [70].

3.2. Simulations of the acid gas removal plant

A possible scheme for the purification section has been studied in this work, in order to meet all the required specifications both for the purified gas and for the CO_2-rich stream to be stored.

Fig. 3 shows the general simplified schematic of the AGR unit for IGCC plants with CO_2 capture (in cases without CO_2 capture, only the H_2S unit is present). For the H_2S removal section, two absorption columns are used, while only one distillation column is enough to regenerate the amine solvent. For the CO_2 capture section, two parallel trains constituted by an absorption and a stripping section each are adopted.

3.3. Removal of hydrogen sulphide

The scheme of the H_2S removal section is shown in Fig. 4.

The H_2S removal section is composed of two absorption columns (Fig. 4 shows only one column, for the sake of simplicity), operating at high pressure, and one distillation column for solvent regeneration, operating at atmospheric pressure.

After cooling, the syngas stream (1,2) enters the acid gas removal plant. Before feeding the absorption column, it is mixed with a compressed recycle stream from the Claus plant (1,3), which contains 4% of the H_2S absorbed (i.e. a sulphur recovery efficiency of 96% has been assumed in the Claus unit). The recycle allows recovering the CO_2 co-absorbed in the H_2S absorber and the unrecovered sulphur in the hydrogenated Claus tail gas, without an additional dedicated amine scrubbing unit. The lean solution (1,15) is used to remove most of the H_2S contained in the stream (1,4). In the cases with CO_2 capture, where most of the H_2S leaving this process unit is captured in the following CO_2 absorption unit, H_2S removal efficiency is determined in order to leave no more than 200 ppm(v) of H_2S in the CO_2-rich stream sent to storage. Considering the target CO_2 capture efficiency of 95%, an

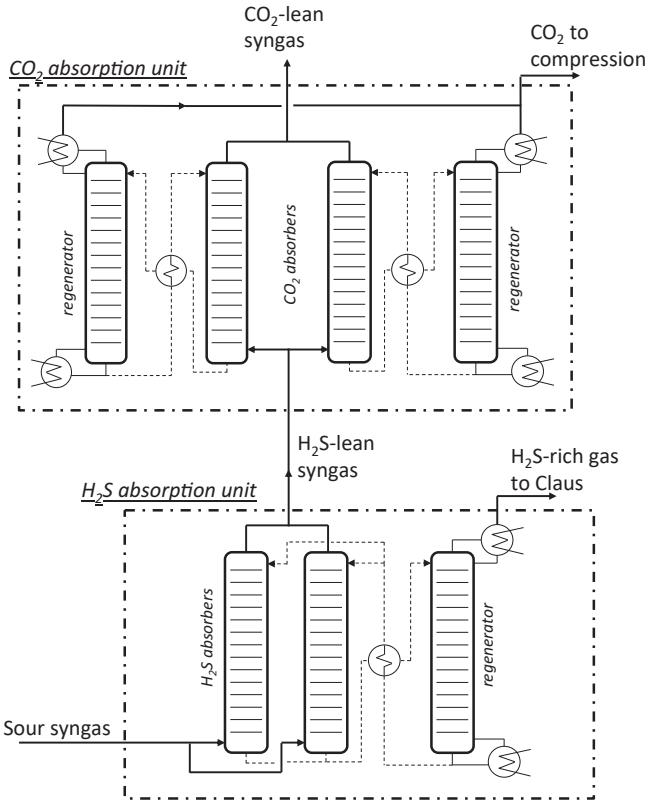

Fig. 3. Scheme of the AGR unit for H_2S and CO_2 separation.

H_2S removal efficiency of about 97.5% and 99.6% is required for the low-sulphur and the high-sulphur coal respectively. In the cases without CO_2 capture, the H_2S separation efficiency is determined in order to achieve a H_2S mole fraction lower than 20 ppm(v) on a dry basis, corresponding to a H_2S separation efficiency of 97.8% and 99.7%, depending on the type of coal used. The lean solution (1,15) is fed to the top of the absorption column and exits rich in H_2S (1,6). The regeneration takes place both in a flash unit (Flash) and in a distillation column: the separator allows the recovery of part of the co-absorbed CO_2 before sending the amine to the distillation column by simply lowering the pressure, with no addition of heat. In the distillation column the rich amine solution and the liquid output from the partial condenser, which is totally recycled to the column, flow from the top trays to the bottom and to the reboiler.

A recuperative heat exchanger transfers heat from the warm regenerated lean solution (1,12) exiting the reboiler of the distillation column to the cold rich solvent (1,9), reducing the amount of heat required in the reboiler.

A make-up of amine solution is added before recycling it to the absorption column after cooling and pumping the solvent to the absorber pressure. The stream rich in H_2S (1,11) is recovered from the partial condenser of the distillation column and fulfills the characteristics for being fed to a Claus plant, assuming a minimum H_2S content of 20 vol.% [41].

Table A4 in the Appendix reports the main characteristics of the H_2S removal section. As anticipated, two absorption columns have been considered for all the cases. The gas flowrate is very high, while the amount of amine solution is much lower. Large columns (necessary to treat the overall gas flowrate) would cause an unbalanced distribution of the liquid along the trays with a low performance of the absorber. Therefore, the feed flowrate has been split into two streams to two identical absorption columns. The diame-

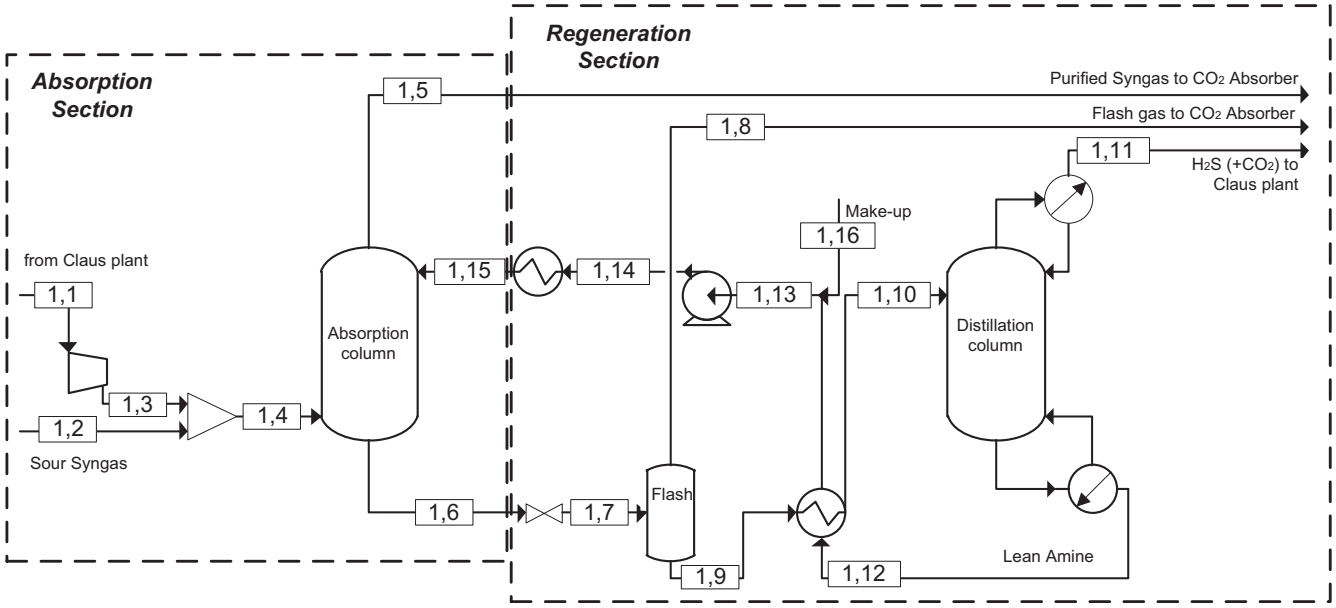

Fig. 4. Scheme of the H_2S removal section.

ter of each absorber has been determined by considering gas velocities of 0.6 m/s, as usually done for mid-pressure columns [71] and by considering also an acceptable hold-up in each tray in order to avoid excessive CO_2 co-absorption for the cases with CO_2 capture. For each case, the highest flowrate (located at the bottom of the absorber) has been considered and the diameter has been determined. A check of the flooding velocity has shown that the considered gas velocity is acceptable (the flooding factors are approximately equal or lower than 0.8).

The number of trays of each absorber has been determined by analyzing the performance of the absorber for a given flow rate and different number of stages.

Figs. 5 and 6 show the results obtained for the C-D-SOA and the C-I-SOA cases, taken as examples of cases characterized by significantly different H_2S content and L/G. The trend of the H_2S mole fraction tends to reach an asymptotic value as the number of trays increases. The final value (12 trays) has been chosen by considering the marginal benefits of an additional stage reduce significantly.

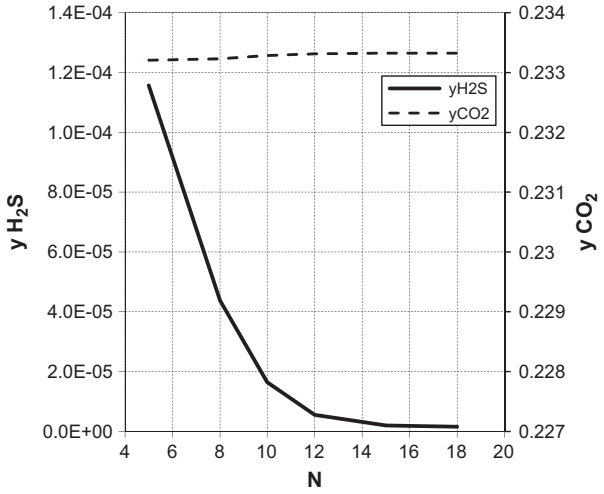

Fig. 6. Mole fractions of H_2S and CO_2 in the purified gas for the C-I-SOA case, obtained by varying the number of trays (N) in the absorption column.

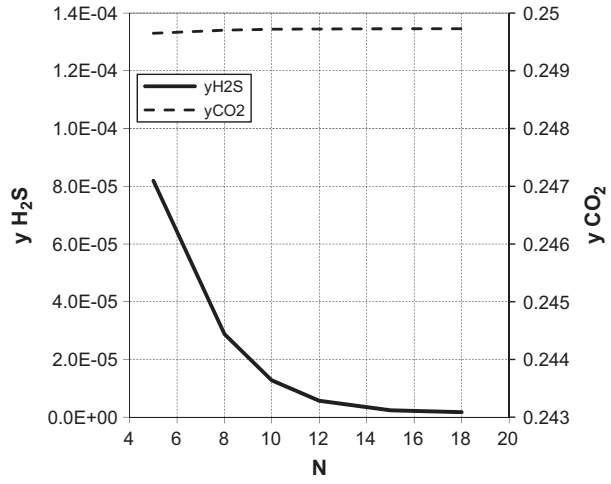

Fig. 5. Mole fractions of H_2S and CO_2 in the purified gas for the C-D-SOA case, obtained by varying the number of trays (N) in the absorption column.

Similar considerations have been done for all the analyzed cases, though not shown here for the sake of brevity.

Table 3 reports the characteristics of the lean amine solvent fed for H_2S removal. The amount of aqueous solution and the concentration of the amine in the solvent have been determined to remove H_2S with low CO_2 co-absorption, in order to obtain an acid gas stream that fulfills the minimum H_2S concentration assumed for feeding the Claus plant. The lean loadings have been determined to have a content in H_2S in the lean solvent exiting the distillation column of $0.18 \cdot 10^{-2}$ mol of H_2S per mole of MDEA. The CO_2 content is a consequence of the removal of the acid gases at the conditions of the regeneration sections and varies depending on the overall amount of co-absorbed CO_2 for each case. Through this value of the lean loading, the heat duty of the stripper is determined.

In order to limit the CO_2 absorption, whose rate of reaction is slower than the one of H_2S, short contact times (obtained by reducing the diameter of the column to limit the hold-up on each tray)

Table 3
Characteristics of the lean amine solvent for H_2S removal.

	C-D-SOA	C-D- ADV	C-I- SOA	C-I- ADV	N-D- SOA	N-D- ADV	N-I- SOA	N-I- ADV
Pressure, bar	29.32	24.11	29.32	24.11	29.32	24.11	29.32	24.11
Temperature, °C	40							
Mass flow rate, kg/s	36	39	275	296	19	21	115	126
L/G	0.19	0.19	1.53	1.48	0.16	0.16	0.98	0.97
MDEA, wt.%	10							
H_2S loading[a], %	0.18							
CO_2 loading[a], %	3.11	3.13	3.89	3.84	2.81	2.86	3.02	3.00
Total loading[a], %	3.28	3.30	4.07	4.02	2.99	3.04	3.20	3.18

[a] Loadings are intended as moles of acid gas per mole of MDEA.

and a low MDEA content in the aqueous solution have been considered. Generally, higher MDEA concentrations are preferred, mainly because of the higher maximum capacity of the loaded solvent [41]. However, some works in the literature [72–75] deal with low concentrations of MDEA solution (as low as 5 wt.%), which have been considered also in this work. An aqueous solution with 10 wt.% MDEA content undergoes to corrosion phenomena similar to the ones for higher concentrated solvents [76], therefore no particular additional material issues would occur in its employment. Since a 10 wt.% MDEA – 90 wt.% H_2O solvent can give the desired selective removal with an acceptable duty at the reboiler of the regeneration section, it has been chosen for the cases under study in this work.

A sensitivity analysis has been performed to select the amine flow rate, as shown in Fig. 7 and in Fig. 8. They refer to two cases with CO_2 capture and to both the coals in Table 1.

As the amine flowrate increases, i.e. with higher L/G, both the amounts of absorbed H_2S and CO_2 increase. The smaller increase

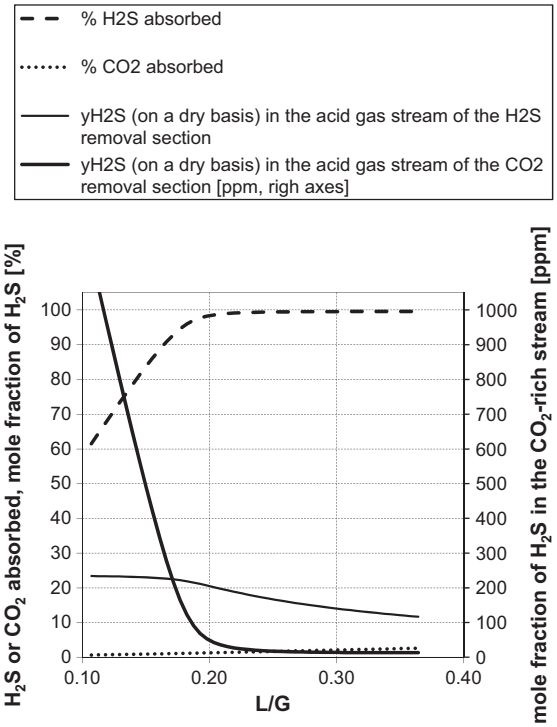

Fig. 7. Amount of absorbed H_2S and co-absorbed CO_2, mole fraction of H_2S (on a dry basis) in the acid gas stream to be sent to a Claus plant and mole fraction of H_2S (on a dry basis) in the acid gas stream exiting the following CO_2 removal section (forecasted if 95% of CO_2 is absorbed) obtained by varying the total amine flowrate for case C-D-SOA.

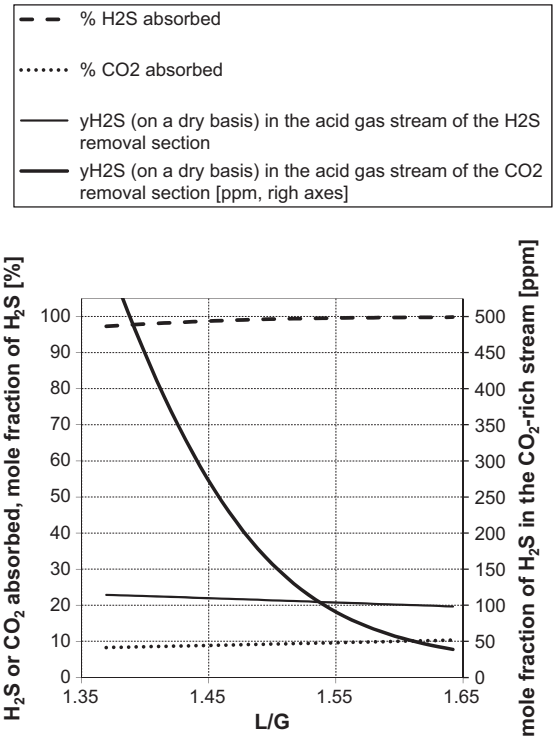

Fig. 8. Amount of absorbed H_2S and co-absorbed CO_2, mole fraction of H_2S (on a dry basis) in the acid gas stream to be sent to a Claus plant and mole fraction of H_2S (on a dry basis) in the acid gas stream exiting the following CO_2 removal section (forecasted if 95% of CO_2 is absorbed) obtained by varying the total amine flowrate for case C-I-SOA.

in percentage of CO_2 corresponds to a non-negligible increase of the CO_2-to-H_2S ratio in the stripper off-gas, because the amount of CO_2 in the raw syngas is much higher than the one of H_2S. Therefore, the mole fraction of H_2S (on a dry basis) in the acid gas stream obtained from the regeneration column in the H_2S removal section decreases as the amine flowrate increases. Thus, amine circulation rates higher than 38 kg/s (L/G = 0.2) would not satisfy the specification of the H_2S content of at least 20% in the Claus feed gas for the C-D-SOA case (see Fig. 7). On the contrary, the gaseous stream rich in acid gases exiting the CO_2 capture section should not contain more than 200 ppm of H_2S, so most of H_2S should be removed in the first removal section. Fig. 7 also reports an estimation of the mole fraction of H_2S on a dry basis, showing that this requirement would not be satisfied for flow rates lower than 33 kg/s (L/G = 0.18).

Therefore, as summarized in Fig. 7, the satisfaction of all the specifications for the C-D-SOA case can be obtained only in a very limited range of flowrates, corresponding to L/G between 0.18 and

Table 4
Main results of acid gas removal by means of a 10 wt.% or a 50 wt.% MDEA aqueous solution in order to achieve a H_2S content in the purified syngas less than 20 ppm(v) for cases N-I-SOA and N-I-ADV.

	N-I-SOA		N-I-ADV	
MDEA in the solvent, wt.%	10	50	10	50
L/G	0.98	0.48	0.97	0.49
Co-absorbed CO_2, mol%	20.99	30.56	19.34	25.20
H_2S in the stream to the Claus plant (dry basis), mol%	40.89	29.4	42.03	33.93
Total reboiler duty, MW	35.24	56.42	37.16	62.49

Table 5
Reboiler duty required for regeneration of the amine solvent in the H_2S removal section for all the considered cases. The total absorbed H_2S refers to the overall amount of H_2S removed in the absorption column from streams (1,1) and (1,2).

	C-D-SOA	C-D-ADV	C-I- SOA	C-I- ADV	N-D- SOA	N-D- ADV	N-I- SOA	N-I- ADV
L/G	0.19	0.19	1.53	1.48	0.16	0.16	0.98	0.97
Total reboiler duty, MW	9.19	10.01	66.51	72.7	5.24	5.77	35.24	37.16
H_2S removal efficiency, %	97.66	97.21	99.70	99.46	99.09	98.83	99.73	99.71
Total absorbed H_2S, kg/s	0.23	0.25	1.55	1.72	0.20	0.22	1.34	1.48
Reboiler duty, $MJ/kg_{absorbed\ H_2S}$	40.50	39.66	42.95	42.32	26.51	26.64	26.25	25.11
H_2S in the stream to the Claus plant (dry basis), mol%	21.10	21.66	20.63	21.23	38.05	37.96	40.89	42.03
H_2S in the CO_2 stream to storage (dry basis), ppm	96	123	157	184				

0.20). This is mainly due to the very low amount of H_2S present in the sour syngas and to the very high CO_2 content, which causes a high CO_2 co-absorption. A solvent circulation rate of 36 kg/s (L/G = 0.19) has been hence selected for the C-D-SOA case.

The syngas obtained from the Illinois #6 coal gasification is characterized by a higher content in H_2S (about 7 times higher) than the syngas from the Douglas Premium coal. Though being the CO_2-to-H_2S ratio very high also in this case, the specification of the H_2S content in the Claus feed and in the CO_2-rich stream can be accomplished easily. As shown in Fig. 8, L/G between about 1.48 and 1.61 are suitable to achieve the gas purity specifications. Therefore, the plant can be operated with a higher flexibility, because a variation in the composition of the stream should not cause possible non-attainment of the desired specifications.

These considerations, made for the cases with CO_2 capture and the state-of-the-art combustion turbine can be extended to the corresponding cases with the advanced combustion turbine. The slightly lower pressure of the syngas (see Table 2) simply requires an increased solvent circulation rate (about 4–8% higher).

In cases without CO_2 capture, a syngas stream with a moderate CO_2 content is treated, due to the absence of WGS reactors. Therefore, in the cases with low CO_2 content, the total circulation rate of the solvent necessary for H_2S removal is much lower than the one of the corresponding case with high CO_2 content (see Table 3), since few CO_2 is co-absorbed.

Due to the increased H_2S-to-CO_2 ratio, the desired removal could be achieved by using a traditional 50 wt.% MDEA aqueous solution. This helps in reducing the amine circulation rate, though decreasing the selectivity to H_2S removal. As a matter of fact, up to about 30% of the inlet CO_2 is co-absorbed in the same column, but being the inlet CO_2 content in the syngas relatively low, the H_2S concentration in the Claus plant feed is maintained well above the assumed minimum of 20 vol.%.

As reported in Table 4, the use of a solvent composed of 10 wt.% MDEA requires a higher L/G, i.e. a higher amine flowrate (about two times higher). Nevertheless, the amount of co-absorbed CO_2 is reduced, thanks to the lower MDEA content. As a consequence, the heat duty at the reboiler of the regeneration section reduces. As a matter of fact, the separation process can be accomplished without excessive boil-up from the reboiler and reflux ratio from the condenser, avoiding high quantities of solvent (mainly water) being vaporized and condensed. Moreover, the feed to the Claus

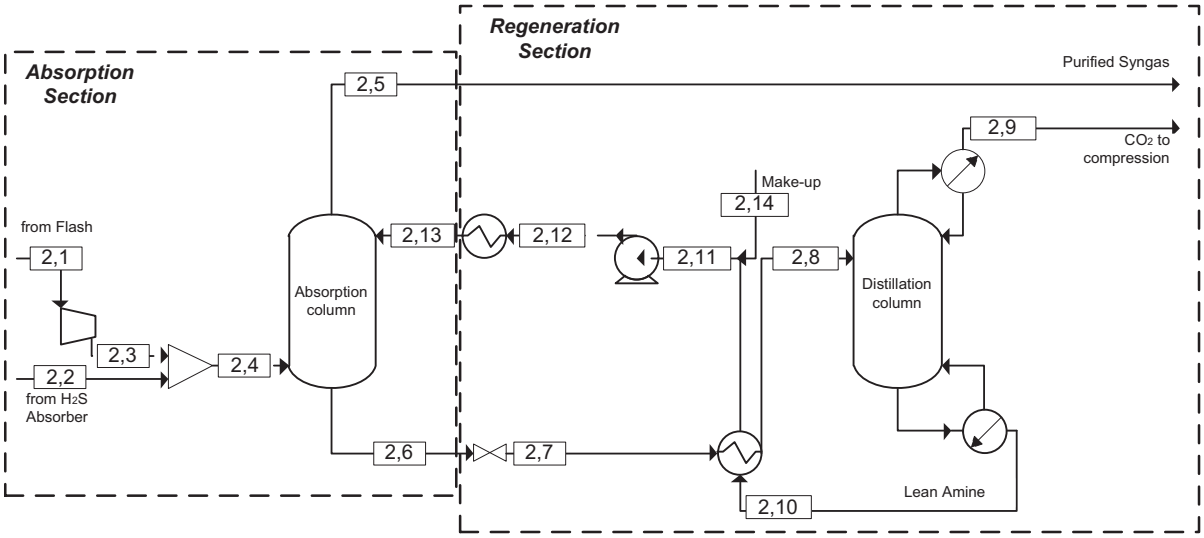

Fig. 9. Scheme of the CO_2 absorption section.

Table 6
Characteristics of the streams fed to the CO_2 absorption section for the cases with CO_2 capture.

	C-D-SOA	C-D-ADV	C-I-SOA	C-I-ADV
Pressure, bar	29.18	23.96	29.13	23.91
Temperature, °C	43.9	43.5	48.4	47.7
Mass flow rate, kg/s	232.93	261.59	217.5	244.04
Component, mol%				
H_2S	$1.88 \cdot 10^{-3}$	$2.15 \cdot 10^{-3}$	$3.54 \cdot 10^{-3}$	$4.42 \cdot 10^{-3}$
CO_2	25.20	25.10	25.11	25.01
H_2O	0.36	0.42	0.43	0.50
CH_4	0.42	0.41	0.45	0.44
CO	0.77	0.74	0.83	0.79
H_2	27.81	27.22	29.16	28.57
N_2	44.91	45.57	43.51	44.16
Ar	0.53	0.54	0.52	0.52

plant obtained by using a 10 wt.% MDEA solution is characterized by a higher H_2S content than the one obtained by using a 50 wt.% MDEA solution. Based on these results, a 10 wt.% MDEA aqueous solution has been employed also for the cases without CO_2 capture.

Table 5 reports the reboiler duty and the removed H_2S for all the assessed cases. The overall heat duty is not very significant if compared to the one required in the CO_2 capture section, but the specific heat (MJ necessary per kg of absorbed H_2S) is very high. This is due to the co-absorption of CO_2 and to the related low amount of H_2S present in stream (1,11). With this regard, it can be appreciated that cases with CO_2 capture feature higher specific duty per kg of absorbed H_2S, due to the higher CO_2 co-absorbed.

3.4. Capture of carbon dioxide

For the cases with CO_2 capture, the H_2S removal section is followed by a CO_2 capture section. Fig. 9 shows the scheme of this section, fed with two streams rich in CO_2, (2,1) and (2,2) exiting the H_2S removal section (corresponding to streams (1,8) and (1,5) in Fig. 4), which are mixed before feeding the absorption column. Characteristics of stream (2,4) are reported in Table 6.

As schematized in Fig. 9, stream (2,1), (or (1,8) in Fig. 4), is compressed to the same pressure of stream (2,2) ((1,5) in Fig. 4) and mixed to it before feeding the absorption column. The MDEA solvent, composed of 50 wt.% MDEA and 50 wt.% H_2O, enters the top of the absorption column with the aim of removing 95% of the CO_2 contained in the stream entering the acid gas removal plant (i.e. stream (1,2) in Fig. 4). Solvent regeneration is performed in a distillation column operating at atmospheric pressure, after recuperative pre-heating in a heat exchanger, in order to recover part of the heat content from the lean amine solution and to save energy in the regeneration process.

The gaseous stream (2,5) exiting the absorption column is the purified syngas sent to the combustion turbine, while stream (2,9) contains mainly CO_2 (always more than 99% on a dry basis) with minor amounts of other gases and less than 200 ppm(v) of H_2S. Stream (2,9) is then compressed to storage.

Table A5 in the Appendix reports the characteristics of the columns of the considered capture section.

The mass flow rate of acid gas (mainly CO_2) to be removed is very high (see Table 6), so the amounts of solvent to be used are expected to be much larger than the ones employed for H_2S removal. Therefore, larger diameters could be used without negative effects on the distribution of the liquid on the tray. By considering other industrial amine scrubbers operating in the natural gas field and treating similar flow rates, a value of 6 m has been chosen for the column diameter. A check on pressure drops and flooding factors has been made as well.

Following the analysis done for the H_2S scrubbers, the number of trays of the absorption section has been set. Moreover, based on the number of trays, higher than for the H_2S absorbers, a check

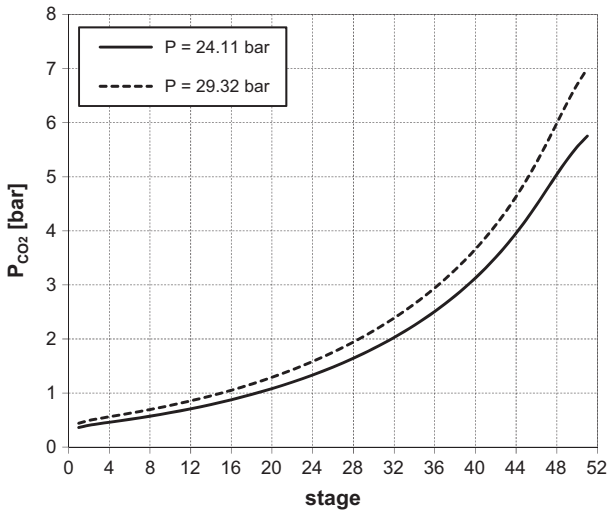

Fig. 10. CO_2 partial pressure at the gas-liquid interface along the absorption column for the cases C-I-SOA (P = 29.32 bar) and C-I-ADV (P = 24.11 bar).

of the height of the column has been done, considering 53 m as a limit for the tower height, as suggested by Walas [71].

The syngas entering the AGR plant of the IGCC with the advanced combustion turbine (cases C-D-ADV and C-I-ADV) is characterized by a composition similar to the state-of-the-art combustion turbine cases (cases C-D-SOA and C-I-SOA), but with a slightly larger flow rate and a lower pressure (see Table 6). These two features have little effect on the design of the H_2S removal section, but strongly influence CO_2 absorption. As a matter of fact, the CO_2 partial pressure is lower, both in the bulk of the vapor phase and at its interface with the liquid phase (see Fig. 10). The CO_2 partial pressure at the interface is related to the amount of CO_2 in the liquid phase, which is in vapor-liquid equilibrium with the vapor phase at the interface.

Fig. 11 shows the profiles of the difference between the CO_2 molar fraction at the interface and the one in the bulk of the liquid phase along the designed absorption columns for cases C-I-SOA and C-I-ADV. The lower the CO_2 partial pressure, the lower the driving force for mass transfer, which strongly affects the difference of CO_2 molar fraction. In order to satisfy the purification specification for the two cases, with an overall CO_2 absorption of 95%, higher amine flow rates and higher residence times are necessary for cases operating at lower pressure (C-D-ADV and C-I-ADV cases). Moreover, being the volumetric vapor flow rates of the cases with the advanced combustion turbine about 20% larger,[1] a

[1] As further explained in the following, the absolute size of the plants is determined by the size of the combustion turbine.

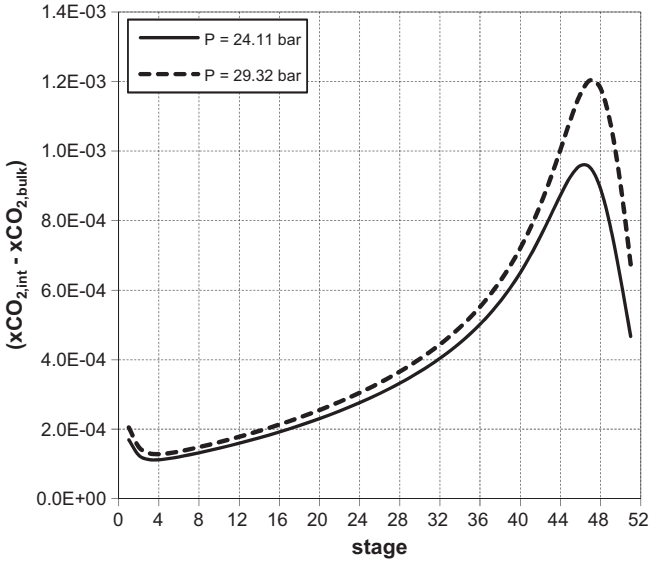

Fig. 11. Difference of CO_2 molar fraction at the interface and the one in the bulk of the liquid phase along the absorption column for the cases C-I-SOA (P = 29.32 bar) and C-I-ADV (P = 24.11 bar).

Table 7
Characteristics of the lean amine solvent for CO_2 capture.

	C-D-SOA	C-D-ADV	C-I-SOA	C-I-ADV
Pressure, bar	29.32	24.11	29.32	24.11
Temperature, °C	40			
Total mass flow rate, kg/s	1618	1884	1500	1760
L/G	2.73	2.84	2.67	2.81
MDEA, wt.%	50			
H_2S loading, %	0.02			
CO_2 loading, %	2.04			
Total loading, %	2.06			

different dimension of the column is selected. Therefore, four parallel absorbers have been used in these cases, each one treating one fourth of the syngas flow rate. This solution can give acceptable residence times, similar to the ones of a column composed of 51 + 51 = 102 trays. It does not exceed the suggested maximum tower height [71] nor the maximum column diameter (about 6 m), as usually found [77]. However, the lower number of trays (51) of the considered columns can limit the separation due to vapor-liquid equilibrium, so a higher circulation rate would be necessary for a given CO_2 capture.

Table 7 reports the characteristics of the lean amine solution used to achieve the desired CO_2 capture.

The stripper duty is determined to obtain a target loading of the regenerated solvent. The solvent flow rate has been chosen in order to remove at least 95% of the CO_2 present in the syngas stream entering the acid gas removal plant. Figs. 12 and 13 show a comparison between the performance obtained with 10 wt.% MDEA and with 50 wt.% MDEA solutions respectively for case C-D-SOA. In case of the 10 wt.% MDEA aqueous solution, solvent circulation higher than the assessed ones would be necessary to achieve the desired 95% CO_2 removal. In the range of L/G considered, the specific heat duty at the reboiler is constant (about 3.6 MJ/kg_{CO_2}), indicating that the solvent exits the absorption column saturated of CO_2. In any case, the specific heat duty obtained is much higher than in the case with more concentrated MDEA solution, indicating that for CO_2 separation from high CO_2 content syngas, a concentrated solvent helps in reducing the circulation rate and the related costs.

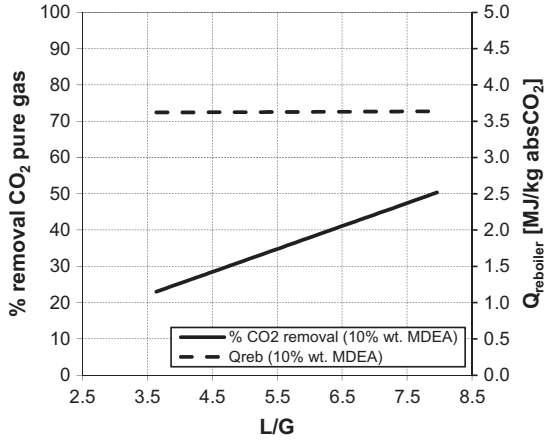

Fig. 12. Amount of CO_2 removal and reboiler duty vs. L/G obtained with flow rates of a 10 wt.% MDEA solution in the range between 680 and 1500 kg/s, according to simulations of the CO_2 capture section for case C-D-SOA.

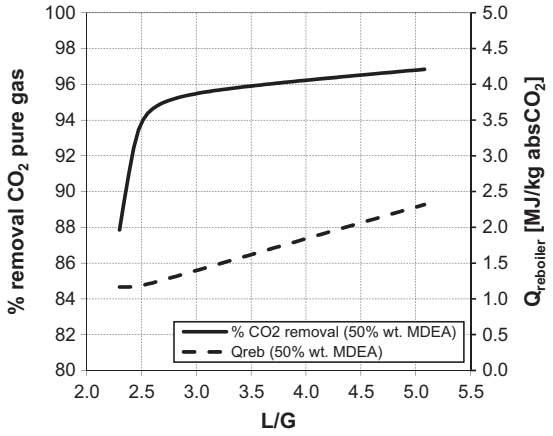

Fig. 13. Amount of CO_2 removal and reboiler duty vs. L/G obtained with flow rates of a 50 wt.% MDEA solution in the range between 680 and 1500 kg/s, according to simulations of the CO_2 capture section for case C-D-SOA.

Considering the 50 wt.% MDEA solution (Fig. 13), the target 95% CO_2 capture can be achieved with L/G of 2.73 and specific heat duty of 1.28 MJ/kg_{CO_2}. This heat duty is close to the minimum value for the assumed operating conditions, that would be achieved for L/G of 2.5 or lower, where the MDEA solution from the absorber is saturated with CO_2.

A sensitivity analysis has been carried out to evaluate the effects of the stripper operating pressure. For a given lean solvent loading, higher bottom temperatures are required if stripping column pressure increases. On the other hand, columns with smaller diameters could be built, a distillate stream with a lower water content and at higher pressure can be recovered, reducing the electric consumptions for CO_2 compression. As CO_2 compression accounts for a significant part of the energy required in a CO_2 capture system, reducing the power for CO_2 compression could compensate the increased penalty associated to the higher heat demand at higher temperature. Another important design parameter is the minimum temperature difference in the lean-rich solution heat exchanger. The optimal $\Delta T_{approach}$ has to be defined on the basis of economic considerations as the best compromise between capital cost (for which a higher ΔT would be preferred) and operating cost (which are reduced when ΔT is reduced).

Three pressure levels (1, 2 and 3 bar) and two different $\Delta T_{approach}$ at the recuperative heat exchanger have been consid-

Table 8
Characteristics of the resulting solvent and reboiler duty required for the desired CO_2 capture for case C-I-SOA at different operating pressures of the distillation column and temperature approach in the lean-rich solution heat exchanger.

Regeneration pressure, bar	1	2	3
Temperature, °C	102.3	122.9	135.1
Total solvent mass flow rate, kg/s	1500	1468	1468
L/G	2.67	2.62	2.62
MDEA, wt.%		50	
H_2S mole fraction in the liquid phase	$3.15 \cdot 10^{-5}$	$3.11 \cdot 10^{-5}$	$3.56 \cdot 10^{-5}$
CO_2 mole fraction in the liquid phase	$2.7 \cdot 10^{-3}$	$1.9 \cdot 10^{-3}$	$1.9 \cdot 10^{-3}$
Reboiler duty ($\Delta T_{approach}$ = 5 K), MJ/$kg_{absorbed\ CO_2}$	1.15	1.17	1.21
Reboiler duty ($\Delta T_{approach}$ = 10 K), MJ/$kg_{absorbed\ CO_2}$	1.26	1.26	1.29

ered. Usually, a difference in temperature approach of 10 K is used as a rule of thumb [71] and assumed in this work for the base case. Cases with $\Delta T_{approach}$ of 5 K, which is a reasonable value in liquid-liquid heat exchangers, have then been considered.

Only the results for the C-I-SOA case are detailed in Table 8, as representative of all the obtained results. In this table, the considered operating conditions, the molar fraction of acid gases in the lean amine solution and the solvent circulation rate are summarized. The heat required at the reboiler for different temperature approaches in the recuperative heat exchanger is reported as well.

The solvent flow rate depends on the lean loading, the ratio between the amount of acid gases over the one of MDEA (on a molar basis) in the liquid. By varying the pressure, the H_2S-to-CO_2 ratio changes because of vapor-liquid equilibrium and so the relative CO_2/H_2S loading of the regenerated solvent. With this regard, the target CO_2 loading, through which the regenerator duty is also determined, has been reduced at higher pressures to achieve a proper solvent regeneration, that would otherwise leave too much of H_2S in the lean solvent. Thus, a different amount of amine solution is needed for a specified level of CO_2 capture, resulting in lower L/G at higher pressures.

As expected, the reboiler duty increases with the pressure and by increasing the approach temperature difference. Reboiler temperature also increases with pressure, requiring steam at higher pressure to be extracted from the turbine for solvent regeneration. Table 9 reports the results obtained when considering in the recuperative heat exchanger the two temperature approach differences (5 K and 10 K) with the pressure at the distillation column set at 1 bar. The heat required at the reboiler decreases by about 9% if $\Delta T_{approach}$ is reduced to 5 K.

3.5. Compression of carbon dioxide

The Peng-Robinson equation of state was used for the simulation of the CO_2 compression station in ASPEN Plus®. An intercooled compression up to 80 bar (calculated assuming 85% of isentropic efficiency, 94% of mechanical-electric efficiency, and 30 °C of intercooling temperatures) with intermediate water adsorption, followed by liquid CO_2 pumping to 110 bar has been considered. Five intercooled compression sections have been adopted for cases with stripper pressure of 1 and 2 bar, leading to specific electric consumptions of 343.8 kJ/kg_{CO_2} and 281.1 kJ/kg_{CO_2} respectively, including auxiliary consumptions for heat rejection to the environment in intercoolers. In the cases with stripper pressure of 3 bar, four compression sections have been considered, leading to specific consumption of 249.8 kJ/kg_{CO_2}. An additional intercooling step in this case would lead to energy savings of only 1.2%.

4. Discussion of IGCC performance

The results of the calculations of the IGCC plants are reported in this section and discussed with reference to the key performance indicators. In addition to the electric efficiency η and the specific

Table 9
Reboiler duty required for amine solvent regeneration at 1 bar in the CO_2 capture section (absorbed CO_2 set at 95%).

	C-D- SOA	C-D-ADV	C-I-SOA	C-I-ADV
Total reboiler duty ($\Delta T_{approach}$ = 5 K), MW	115.54	132.66	107.24	123.89
Total reboiler duty ($\Delta T_{approach}$ = 10 K), MW	126.82	145.71	117.68	136.13
Total absorbed CO_2, kg/s	99.06	110.12	93.61	103.99
Reboiler duty ($\Delta T_{approach}$ = 5 K), MJ/$kg_{absorbed\ CO_2}$	1.17	1.20	1.15	1.19
Reboiler duty ($\Delta T_{approach}$ = 10 K), MJ/$kg_{absorbed\ CO_2}$	1.28	1.32	1.26	1.31

Table 10
Power balances and main overall performance indicators of the reference IGCC plants without CO_2 capture.

	N-D-SOA	N-D-ADV	N-I-SOA	N-I-ADV
CT power, MW_{el}	228.0	271.8	228.6	272.9
CT auxiliaries, MW_{el}	−0.80	−0.95	−0.80	−0.96
Steam turbine, MW_{el}	239.4	257.9	232.7	250.5
Steam cycle pumps, MW_{el}	−6.34	−6.76	−6.09	−6.49
Air separation unit, MW_{el}	−10.21	−11.43	−9.41	−10.52
Lock hopper compressors, MW_{el}	−10.47	−11.09	−9.65	−10.21
Air booster, MW_{el}	−19.67	−16.14	−18.16	−14.88
Auxiliaries for H_2S removal, MW_{el}	−0.27	−0.27	−1.65	−1.58
Other IGCC auxiliaries, MW_{el}	−3.57	−3.94	−3.46	−3.81
Heat to H_2S stripper, MW_{th}	5.24	5.77	35.24	37.16
Overall net power, MW_{el}	416.0	479.1	412.1	475.0
Heat input, MW_{LHV}	867.4	957.7	879.9	970.8
LHV cold gas efficiency	74.96%	74.18%	73.79%	73.07%
LHV gross efficiency	53.87%	55.31%	52.42%	53.92%
LHV net efficiency	47.96%	50.03%	46.83%	48.93%
Specific emissions, kg_{CO_2}/MW h	725.2	694.8	675.9	647.7

emissions *ER*, the specific primary energy consumption for CO_2 avoided (SPECCA) is calculated for the plants with CO_2 capture, according to Eq. (12).

$$SPECCA = \frac{3600 \cdot \left(\frac{1}{\eta} - \frac{1}{\eta_{ref}}\right)}{ER_{ref} - ER} \quad (12)$$

where "*ref*" indicates the index of the reference IGCC without capture, using the same coal and the same combustion turbine technology.

The size of all the plants assessed is determined by the combustion turbine. The syngas production has to match with the combustion turbine size, which is characterized by a given exhaust gas flow rate of 665 kg/s.

4.1. IGCC plants without CO_2 capture

The main results of the reference IGCC plants without CO_2 capture are reported in Table 10.

The CT technology strongly affects the IGCC performance: efficiency gains higher than 2% points are obtained with the advanced technology. This is mainly due to the higher efficiency of the combined cycle, which is evident from the higher plant gross efficiency (by about 1.5% points), and to the lower penalty associated to the air booster, consequence of the lower fuel overpressure required at the combustor inlet. The coal quality also significantly affects the performance of the plants. The net efficiency of IGCCs fed with the high-sulphur coal is 1% point lower, as a result of the much larger heat duty required for AGR solvent regeneration.

4.2. IGCC plants with CO_2 capture

The main results for the IGCC plants with CO_2 capture are reported in Tables 11–14. In detail, six sets of results are reported for each IGCC plant, resulting from calculations with the three CO_2 stripping pressures and the two $\Delta T_{approach}$ values at the recuperative heat exchanger, as anticipated in Section 3.4.

Table 11
Power balances and main overall performance for the IGCC plants with CO_2 capture (cases C-D-SOA: gasification of Douglas Premium coal and use of the state-of-the-art combustion turbine).

Regeneration pressure, bar	1		2		3	
$\Delta T_{approach}$, K	5	10	5	10	5	10
CT power, MW_{el}	227.2					
CT auxiliaries, MW_{el}	−0.80					
Steam turbine, MW_{el}	243.8	241.6	236.8	234.6	233.9	231.7
Steam cycle pumps, MW_{el}	−5.79	−5.69	−5.74	−5.66	−5.75	−5.68
Air booster, MW_{el}	−32.72					
Auxiliaries for H_2S removal, MW_{el}	−0.65					
Auxiliaries for CO_2 capture, MW_{el}	−3.17	−3.31	−3.21	−3.34	−3.26	−3.40
Other IGCC auxiliaries, MW_{el}	−5.11					
CO_2 compression, MW_{el}	−34.02		−27.81		−24.71	
Heat for H_2S stripping, MW_{th}	9.19					
Heat for CO_2 stripping, MW_{th}	115.4	126.7	121.8	130.4	123.4	131.8
Overall net power, MW_{el}	388.7	386.5	388.0	385.8	388.1	385.8
Heat input, MW_{LHV}	1018.6					
LHV cold gas efficiency	67.11%					
LHV gross efficiency	46.24%	46.03%	45.55%	45.34%	45.27%	45.05%
LHV net efficiency	38.17%	37.95%	38.09%	37.87%	38.10%	37.88%
Efficiency penalty, % points	−9.79	−10.01	−9.87	−10.08	−9.85	−10.08
Specific emissions, kg_{CO_2}/MW h	96.18	96.73	96.39	96.93	96.35	96.91
SPECCA, MJ/kg_{CO_2}	3.06	3.15	3.09	3.18	3.09	3.18

Table 12
Power balances and main overall performance for the IGCC plants with CO_2 capture (cases C-D-ADV: gasification of Douglas Premium coal and use of the advanced combustion turbine).

Regeneration pressure, bar	1		2		3	
$\Delta T_{approach}$, K	5	10	5	10	5	10
CT power, MW_{el}	276.3					
CT auxiliaries, MW_{el}	−0.97					
Steam turbine, MW_{el}	261.1	258.4	253.7	251.1	249.8	247.1
Steam cycle pumps, MW_{el}	−6.04	−5.92	−6.03	−5.94	−6.02	−5.93
Air booster, MW_{el}	−27.85					
Auxiliaries for H_2S removal, MW_{el}	−0.63					
Auxiliaries for CO_2 capture, MW_{el}	−3.15	−3.32	−3.23	−3.39	−3.29	−3.46
Other IGCC auxiliaries, MW_{el}	−5.63					
CO_2 compression, MW_{el}	−37.72		−30.83		−27.40	
Heat for H_2S stripping, MW_{th}	10.01					
Heat for CO_2 stripping, MW_{th}	132.1	145.2	135.8	146.3	140.2	150.2
Overall net power, MW_{el}	455.4	452.7	454.8	452.2	454.3	451.5
Heat input, MW_{LHV}	1128.2					
LHV cold gas efficiency	66.22%					
LHV gross efficiency	47.63%	47.39%	46.98%	46.75%	46.64%	46.40%
LHV efficiency	40.37%	40.12%	40.32%	40.08%	40.27%	40.03%
Efficiency penalty, % points	−9.66	−9.91	−9.71	−9.95	−9.76	−10.00
Specific emissions, kg_{CO_2}/MW h	89.75	90.30	89.87	90.40	89.96	90.51
SPECCA, MJ/kg_{CO_2}	2.85	2.94	2.87	2.96	2.88	2.97

Table 13
Power balances and main overall performance for the IGCC plants with CO_2 capture (cases C-I-SOA: gasification of Illinois #6 coal and use of the state-of-the-art combustion turbine).

Regeneration pressure, bar	1		2		3	
$\Delta T_{approach}$, K	5	10	5	10	5	10
CT power, MW_{el}			228.1			
CT auxiliaries, MW_{el}			−0.80			
Steam turbine, MW_{el}	233.8	231.6	225.8	223.8	221.6	219.5
Steam cycle pumps, MW_{el}	−5.30	−5.20	−5.30	−5.23	−5.30	−5.24
Air booster, MW_{el}			−30.12			
Auxiliaries for H_2S removal, MW_{el}			−4.42			
Auxiliaries for CO_2 capture, MW_{el}	−3.59	−3.72	−3.64	−3.77	−3.69	−3.82
Other IGCC auxiliaries, MW_{el}			−4.93			
CO_2 compression, MW_{el}	−32.14		−26.27		−23.35	
Heat for H_2S stripping, MW_{th}			66.52			
Heat for CO_2 stripping, MW_{th}	107.1	117.5	109.4	117.6	113.2	121.0
Overall net power, MW_{el}	380.6	378.4	378.4	376.3	377.1	374.9
Heat input, MW_{LHV}			1025.5			
LHV cold gas efficiency			66.41%			
LHV gross efficiency	45.03%	44.82%	44.26%	44.06%	43.84%	43.64%
LHV efficiency	37.11%	36.89%	36.90%	36.69%	36.76%	36.56%
Efficiency penalty, % points	−9.72	−9.94	−9.93	−10.13	−10.07	−10.27
Specific emissions, $kg_{CO_2}/MW\,h$	96.17	96.73	96.72	97.26	97.07	97.62
SPECCA, MJ/kg_{CO_2}	3.47	3.57	3.57	3.67	3.64	3.74

Table 14
Power balances and main overall performance for the IGCC plants with CO_2 capture (cases C-I-ADV: gasification of Illinois #6 coal and use of the advanced combustion turbine).

Regeneration pressure, bar	1		2		3	
$\Delta T_{approach}$, K	5	10	5	10	5	10
CT power, MW_{el}			277.2			
CT auxiliaries, MW_{el}			−0.97			
Steam turbine, MW_{el}	249.7	247.1	240.3	237.9	235.5	233.0
Steam cycle pumps, MW_{el}	−5.50	−5.39	−5.51	−5.43	−5.51	−5.44
Air booster, MW_{el}			−25.62			
Auxiliaries for H_2S removal, MW_{el}			−4.26			
Auxiliaries for CO_2 capture, MW_{el}	−3.45	−3.60	−3.52	−3.68	−3.59	−3.75
Other IGCC auxiliaries, MW_{el}			−5.43			
CO_2 compression, MW_{el}	−35.61		−29.11		−25.87	
Heat for H_2S stripping, MW_{th}			72.7			
Heat for CO_2 stripping, MW_{th}	123.4	135.6	126.9	136.7	131.1	140.5
Overall net power, MW_{el}	446.1	443.5	443.1	440.6	441.5	438.9
Heat input, MW_{LHV}			1135.1			
LHV cold gas efficiency			65.57%			
LHV gross efficiency	46.42%	46.20%	45.59%	45.38%	45.17%	44.95%
LHV efficiency	39.30%	39.07%	39.04%	38.82%	38.89%	38.67%
Efficiency penalty, % points	−9.63	−9.86	−9.89	−10.11	−10.04	−10.26
Specific emissions, $kg_{CO_2}/MW\,h$	89.86	90.39	90.46	90.97	90.80	91.33
SPECCA, MJ/kg_{CO_2}	3.23	3.33	3.35	3.44	3.41	3.51

As detailed in the four tables, the CT power output is always the same, as well as the air booster demand and all the power plant auxiliaries but the ones related to the CO_2 capture section. These results are justified as variations of the pressure for CO_2 stripping and/or of the $\Delta T_{approach}$ value of the recuperative heat exchanger reflect on the heat duty for CO_2 stripping (and therefore on the steam turbine power output, the demand of steam cycle pumps and the auxiliaries for CO_2 capture) and the CO_2 compressor work.

On the whole, results show that higher CO_2 stripping pressures lead to lower consumptions for CO_2 compression, which are however balanced by higher penalties on the steam turbine power output. On the whole, LHV efficiency reduces when raising the pressure for CO_2 stripping, independently of the coal input and of the combustion turbine adopted for the topping cycle. This LHV efficiency reduction is very small for cases with Douglas Premium coal, while it is more significant in case of Illinois #6 coal input, for which penalties of about 0.4% points have been calculated when the stripper pressure is raised from 1 to 3 bar. This is due to the fact that a single steam extraction point has been considered in the steam turbine for both H_2S and CO_2 strippers. Since the H_2S stripper is always operated at atmospheric pressure, using steam at higher pressure in the H_2S stripping column does not involve any energy benefit, but just a higher penalty for the steam cycle performance. This additional penalty is therefore higher when a high-sulphur coal is used, requiring a higher duty in the H_2S stripper.

As for the minimum temperature difference in the lean-rich solvent heat exchanger, the lower the $\Delta T_{approach}$ the better the overall IGCC performance, in spite of the pressure set for CO_2 stripping. A difference in LHV efficiency of 0.20–0.25% points can be appreciated if reference to the values in Tables 11–14 is made.

On the whole, the efficiency penalty between 9.6 and 10.3% points has been calculated for the cases assessed, with a limited dependence on the type of coal and the combustion turbine technology considered. This penalty is comparable to the one reported in technical literature for dry-feed oxygen-blown IGCCs with pre-combustion CCS technology, ranging from about 8.6% points, as reported by some authors [4,23], to higher values as detailed in EBTF guidelines [38] or in a report by the National Energy Technol-

ogy Laboratory of the U.S. Department of Energy [78] (about 10.2 and 10.9% points, respectively).

The absolute net efficiencies obtained, ranging from 36.6 to 38.2% in case of state-of-the-art combustion turbine and from 38.7 to 40.4% in case of the advanced turbomachinery, demonstrate a high competitiveness from the efficiency point of view of the assessed systems with respect to oxygen-blown gasification plants.

Since all the plants assessed have the same target CO_2 capture efficiency of 95%, SPECCA values reflect the efficiency ones. Values between 2.8 and 3.6 MJ/kg_{CO_2} have been calculated. These values are in line with the SPECCA of 3.14 MJ/kg_{CO_2} calculated for an IGCC plant based on air-blown gasification of a similar low-sulphur coal but with post-combustion CO_2 capture by amine scrubbing [3].

In addition to this analysis and with an eye to possible future technology developments, Tables A6 and A7 in the Appendix detail the main stream characteristics, as numbered in Fig. 1, for the cases C-D-ADV and C-I-ADV. With the exception of stream #25 (steam to AGR section reboilers), all the other data reported in the tables do not vary in case of different CO_2 stripping pressures and $\Delta T_{approach}$ values at the recuperative heat exchanger.

Ultimately, some considerations are made about prospects of possible improvement of the reference MDEA process assessed in this work. As a matter of fact, modifications of the basic configuration of the MDEA process for CO_2 capture may be introduced to reduce the stripper heat duty, which represents the largest source of efficiency penalty of the MDEA process. Alternative configurations have been studied mainly for post-combustion CO_2 capture systems by amine solvents [79,80], with benefits in terms of energy saving. Modifications may involve a single unit or the overall absorption and desorption plant. CO_2 absorption is an exothermic process and the produced heat leads to an increase in the temperature of the solvent, which influences the CO_2 absorption rate and can lower the amount of absorbed acid gas (for a given solvent flow rate). Maintaining the solvent in the column at optimal temperatures for CO_2 absorption may increase the efficiency of the absorption process [79,81]. Other process schemes which employ both lean and semi-lean solvents for acid gas removal in the absorption column have been proposed by other researchers [79,82,83]. For a given CO_2 capture, using a partially regenerated solvent requires a higher amount of amine solution circulating in the system, but allows a pre-removal of carbon dioxide, lowering the amount of vapor flow rate required in the regeneration column for CO_2 stripping. Studies on post combustion capture by Monoethanolamine solvent have shown that a decrease in the reboiler duty higher than 15% can be achieved [84,85]. Moreover, lowering the pressure causes the vaporization of part of the solvent without using any source of energy. This is a way for producing semi-lean solvent from the rich solutions exiting the absorption column [86], which may also be used to produce additional vapor flow rate to be sent for stripping in the regeneration column. In this case, the vapor stream is generated from a lean solution and is then composed mainly of water, which can be compressed and fed to the regenerator as additional stripping steam [87]. Though additional energy is required for compressing the flashed vapors, the net energy requirement of the system is reported to be reduced of about 5% [79].

A detailed study of such schemes for pre-combustion capture is out of the scope of this work, however a theoretical sensitivity analysis is presented in Fig. 14 on the heat duty of the CO_2 stripper of the C-D-SOA case with CO_2 stripping at 1 bar. This analysis aims at quantifying the potential efficiency benefits obtainable by more advanced process configurations, leading to reduced heat duties, without significantly affecting the electric consumptions. A linear increase of efficiency can be found by reducing the reboiler duty from 1.15 MJ/kg_{CO_2} of the base case to 0.6 MJ/kg_{CO_2}, gaining roughly

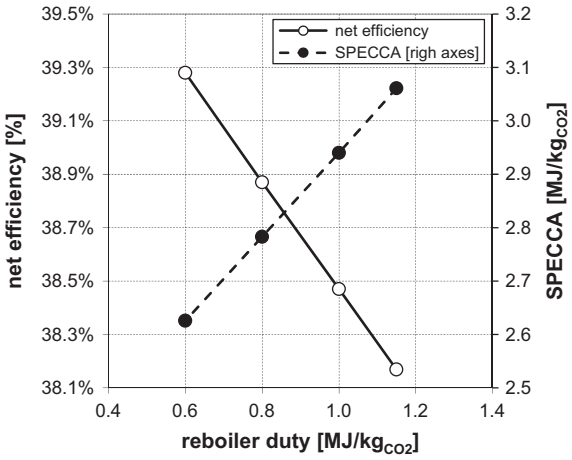

Fig. 14. Effect of reboiler duty on net efficiency and SPECCA of the C-D-SOA case with CO_2 stripping at 1 bar.

0.4% points per 0.2 MJ/kg_{CO_2} saved in the reboiler. The same trend can be appreciated for the SPECCA, for which a decrease of about 0.15 MJ/kg_{CO_2} per 0.2 MJ/kg_{CO_2} saved in the reboiler is obtained.

5. Conclusions

Pre-combustion CO_2 capture by MDEA absorption has been considered as CCS technology for air-blown IGCC plants with the following conclusions.

- Based on the layouts proposed for the acid gas removal plants, the heat duty at the H_2S removal section is always less than 8% of the one necessary for CO_2 stripping in case of low-sulphur coal gasification. However, it is no longer negligible in case of high-sulphur coal, as it can increase up to about 60% of the heat duty for CO_2 stripping.
- As a measure to limit the energy cost related to the adopted CCS technology, the temperature approach in the recuperative heat exchanger of the CO_2 capture section should be as low as possible. Efficiency gain of about 0.20–0.25% points can be obtained by reducing the minimum temperature difference from 10 to 5 K. On the other hand, higher capital cost will be obtained and the optimal temperature difference has to be defined based on an economic optimization calculation.
- The effect of raising the operating pressure of the CO_2 stripping column has been evaluated. As a consequence of the opposite effects on CO_2 compression consumptions and on the losses

Table A1
Main assumptions for CT performance simulation.

	SOA	ADV
Air filter pressure loss, %	1	
Compressor pressure ratio	18.1	
Compressor polytropic efficiency[a], %	90.5	92.5
Compressor leakage, % of the inlet flow	0.75	
Pressure loss in the combustor, %	4	3
Cooled turbine stage isentropic efficiency[a], %	88	91.15
Uncooled turbine stage isentropic efficiency[a], %	90	92.15
Turbine inlet temperature, °C	1305	1360
Fuel valve pressure loss, bar	10	5
Mass flow rate at CT outlet, kg/s	665	
Turbine/compressor mechanical efficiency, %	99.865	
CT auxiliaries, % of gross power	0.35	
Electric generator efficiency, %	98.7	

[a] Efficiency of large compressor and turbine stages. The actual efficiency is calculated by GS built-in correlations as a function of the actual size of the machine.

Table A2
Main assumptions for gasification station calculations (cases with CO_2 capture).

	SOA	ADV
Gasification pressure, bar	37	30.4
Combustor/reductor temperature, °C	1900/1200	
Carbon conversion, %	99.9	
Heat to membrane walls, % of coal LHV input	2	
Pressure/temperature of gasifying air, bar/°C	43.5/541	35.8/495
Air booster polytropic efficiency, %	90.5	
Heat loss in syngas coolers, % of transferred heat	0.7	
Steam-to-CO ratio at HT WGS reactor inlet	1.5	
Overall pressure loss in syngas cooling and treating line, %	24	
Syngas temperature at HT WGS reactor inlet, °C	326.2	318.7
Syngas temperature at LT WGS reactor inlet, °C	210	

Table A3
Main assumptions for HRSC calculations (cases with CO_2 capture).

	SOA	ADV
HRSG gas side pressure loss, kPa	3	
Heat loss, % of transferred heat	0.7	
HP/MP evaporation pressure, bar	144/40	144/36
Maximum live steam temperature, °C	565	
Minimum pinch point ΔT, °C	10	
Subcooling ΔT at drum inlet, °C	5	
Minimum stack temperature, °C	115	
Pressure losses in HP/MP economizers, %	16/25	
Pressure loss in superheaters, %	8	
Condensing pressure, bar	0.04	
Auxiliary electric consumption for heat rejection, MJ_{el}/MJ_{th}	0.01	
Pumps hydraulic efficiency, %	80	
Turbine mechanical efficiency, %	99.5	
Electric generator efficiency, %	98.7	

for steam extraction at higher pressure, net plant efficiency slightly reduces when raising the CO_2 stripping pressure in case of the low-sulphur Douglas Premium coal gasification. The efficiency reduction is more significant (about 0.4% points have been calculated when the stripper pressure is raised from 1 to 3 bar) in case of Illinois #6 coal input, due to the amplified losses associated to H_2S stripping.

- Better IGCC performance is calculated in case of low-sulphur coal gasification, with differences in LHV efficiency ranging from 1.1 to 1.4% points, depending on the two above-mentioned design parameters of the CO_2 capture section. This difference is largely due to the different consumptions for H_2S removal and is present also in the IGCCs without CO_2 capture.
- An advanced combustion turbine technology with higher TIT (1360 °C instead of 1305 °C) may significantly improve the IGCC efficiency, with differences higher than 2% points independently of the coal input and of the adoption of the CO_2 capture unit.
- Efficiency penalties between 9.6 and 10.3% points have been calculated when introducing the CO_2 capture process. Such a penalty can be considered larger if compared to values reported for oxygen-blown gasification IGCCs with CO_2 capture. On the other hand, the absolute net efficiencies obtained, ranging from 36.6 to 38.2% in case of state-of-the-art CT and from 38.7 to 40.4% in case of advanced CT, are highly competitive with oxygen-blown gasification plants from an efficiency point of view.
- Gains of IGCC performance can be obtained by adopting more advanced process configurations, limiting the heat duty of the CO_2 stripper. Such benefits have been quantified for the reference configuration in 0.4% points higher efficiency and 0.15 MJ/kg_{CO_2} lower SPECCA when 0.2 MJ/kg_{CO_2} are saved in the CO_2 reboiler.

Table A4
Characteristics of the main equipment of the H_2S removal section (other common assumptions are related to the lean amine pump, with an efficiency set at 86%, and to the Claus tail gas recycle compressor, with an efficiency set at 72%).

	C-D- SOA	C-D-ADV	C-I- SOA	C-I- ADV	N-D- SOA	N-D- ADV	N-I- SOA	N-I- ADV
Absorption columns	2							
Diameter, m	3.5					2.8		
Trays	12							
Type of tray	Valve							
Pressure at the bottom, bar	29.32	24.11	29.32	24.11	29.32	24.11	29.32	24.11
Pressure of the flash, bar	1.01							
Temperature of the flash, °C	35							
Regeneration columns	1							
Diameter, m	2		5		2		4	
Trays	13							
Type of tray	Valve							
Pressure at the top, bar	1.01							
Condenser	Partial							
Temperature at the condenser, °C	35							

Table A5
Characteristics of the main equipment of the CO_2 capture section.

	C-D-SOA	C-D-ADV	C-I-SOA	C-I-ADV
Absorption columns	2	4	2	4
Diameter, m	6			
Trays	51			
Type of tray	Valve			
Pressure at the bottom, bar	29.18	23.9	29.18	23.9
Regeneration columns	2			
Diameter, m	6			
Trays	8			
Type of tray	Valve			
Pressure at the top, bar	1.01			
Condenser	Partial			
Temperature at the condenser, °C	30			

Table A6
Temperature, pressure, flow rate and composition of the main streams of the IGCC plant shown in Fig. 1 for the case C-D-ADV (CO_2 stripping pressure and $\Delta T_{approach}$ at the recuperative heat exchanger fixed at 1 bar and 10 K).

	T (°C)	p (bar)	ṁ (kg/s)	Ar	CO	CO_2	H_2	H_2O	H_2S	N_2	O_2	CH_4
1	15		44.8				Douglas Premium coal, as received					
2	80	60.87	11.6			100						
3	15	1.01	691.2	0.92		0.03		1.03		77.28	20.73	
4	417.5	18.16	381.9	0.92		0.03		1.03		77.28	20.73	
5	1439.1	17.61	532.1	0.90		1.30		15.74		76.01	6.05	
6	596.5	1.04	665	0.91		1.06		12.95		76.25	8.83	
7	141.4	1.01	665	0.91		1.06		12.95		76.25	8.83	
8	494.6	35.81	176.4	0.92		0.03		1.03		77.28	20.73	
9	1200	30.44	230.6	0.65	26.14	5.18	7.85	3.85	0.08	55.05		0.50
10	900	30.44	226.4	0.66	26.32	5.22	7.90	3.88	0.09	55.44		0.50
11	349	29.83	226.4	0.66	26.32	5.22	7.90	3.88	0.09	55.44		0.50
12	150	29.23	226.4	0.66	26.32	5.22	7.90	3.88	0.09	55.44		0.50
13	358.8	36	51.1					100				
14	210	26.69	281.4	0.48	4.65	18.61	20.59	14.36	0.06	40.88		0.37
15	257.3	25.89	281.4	0.48	0.68	22.58	24.56	10.38	0.06	40.88		0.37
16	150	25.37	281.4	0.48	0.68	22.58	24.56	10.38	0.06	40.88		0.37
17	232.3	23.16	150.2	0.71	1.00	1.65	35.96	0.31		59.84		0.54
18	335	144	50					100				
19	339	144	116					100				
20	565	144	166					100				
21	245	36	9.8					100				
22	560.6	132.48	214.8					100				
23	358.8	36	161.5					100				
24	563.8	33.12	171.3					100				
25	188	2	66					100				

Table A7
Temperature, pressure, flow rate and composition of the main streams of the IGCC plant shown in Fig. 1 for the case C-I-ADV (CO_2 stripping pressure and $\Delta T_{approach}$ at the recuperative heat exchanger fixed at 1 bar and 10 K).

	T (°C)	P (bar)	ṁ (kg/s)	Ar	CO	CO_2	H_2	H_2O	H_2S	N_2	O_2	CH_4
1	15		45.7				Illinoi6 #6 coal, as received					
2	80	60.87	11.8			100						
3	15	1.01	688.4	0.92		0.03		1.03		77.28	20.73	
4	417.5	18.16	393.5	0.92		0.03		1.03		77.28	20.73	
5	1439.1	17.61	532.2	0.90		1.28		15.69		75.63	6.50	
6	596.5	1.04	665	0.90		1.04		12.91		75.94	9.20	
7	143.3	1.01	665	0.90		1.04		12.91		75.94	9.20	
8	494.6	35.81	162	0.92		0.03		1.03		77.28	20.73	
9	1200	30.44	218.3	0.62	24.91	5.58	9.89	5.49	0.58	51.95		0.52
10	900	30.44	215.6	0.62	25.02	5.61	9.94	5.51	0.58	52.20		0.53
11	349	29.83	215.6	0.62	25.02	5.61	9.94	5.51	0.58	52.20		0.53
12	150	29.23	215.6	0.62	25.02	5.61	9.94	5.51	0.58	52.20		0.53
13	358.8	36	45					100				
14	210	26.69	263.7	0.47	4.72	18.48	21.76	14.19	0.44	39.54		0.40
15	257.6	25.89	263.7	0.47	0.72	22.48	25.76	10.20	0.44	39.54		0.40
16	150	25.37	263.7	0.47	0.72	22.48	25.76	10.20	0.44	39.54		0.40
17	232.6	23.16	138.7	0.69	1.06	1.65	37.76	0.31		57.96		0.59
18	335	144	49					100				
19	339	144	111.1					100				
20	565	144	160.1					100				
21	245	36	9.9					100				
22	560.6	132.48	209.7					100				
23	358.9	36	162.6					100				
24	563.8	33.12	172.4					100				
25	188.4	2	88.6					100				

Appendix A.

See Tables A1–A7.

References

[1] Bhattacharya M, Rafiq S, Bhattacharya S. The role of technology on the dynamics of coal consumption–economic growth: new evidence from China. Appl Energy 2015;154:686–95.

[2] Hoffmann BS, Szklo A. Integrated gasification combined cycle and carbon capture: a risky option to mitigate CO_2 emissions of coal-fired power plants. Appl Energy 2011;88:3917–29.

[3] Giuffrida A, Bonalumi D, Lozza G. Amine-based post-combustion CO_2 capture in air-blown IGCC systems with cold and hot gas clean-up. Appl Energy 2013;110:44–54.

[4] Tola V, Pettinau A. Power generation plants with carbon capture and storage: a techno-economic comparison between coal combustion and gasification technologies. Appl Energy 2014;113:1461–74.

[5] Lee JJ, Kim YS, Cha KS, Kim TS, Sohn JL, Joo YJ. Influence of system integration options on the performance of an integrated gasification combined cycle power plant. Appl Energy 2009;86(9):1788–96.

[6] Kim YS, Lee JJ, Kim TS, Sohn JL, Joo YJ. Performance analysis of a syngas-fed gas turbine considering the operating limitations of its components. Appl Energy 2010;87(5):1602–11.

[7] Giuffrida A, Romano MC, Lozza G. Thermodynamic assessment of IGCC power plants with hot fuel gas desulfurization. Appl Energy 2010;87(11):3374–83.

[8] Kunze C, Spliethoff H. Assessment of oxy-fuel, pre- and post-combustion based carbon capture for future IGCC plants. Appl Energy 2012;94:109–16.

[9] Pettinau A, Ferrara F, Amorino C. Techno-economic comparison between different technologies for a CCS power generation plant integrated with a subbituminous coal mine in Italy. Appl Energy 2012;99:32–9.

[10] Mansouri Majoumerd M, Raas H, De S, Assadi M. Estimation of performance variation of future generation IGCC with coal quality and gasification process – simulation results of EU H2-IGCC project. Appl Energy 2014;113:452–62.

[11] Lee HH, Lee JC, Joo YJ, Oh M, Lee CH. Dynamic modeling of Shell entrained flow gasifier in an integrated gasification combined cycle process. Appl Energy 2014;131:425–40.

[12] Kobayashi M, Nakao Y. Inhibition and elimination of carbon deposition in dry gas desulfurization process under oxy-fuel IGCC derived coal gas environment. Fuel 2015;152:19–28.

[13] Promes EJO, Woudstra T, Schoenmakers L, Oldenbroek V, Thallam Thattai A, Aravind PV. Thermodynamic evaluation and experimental validation of 253 MW integrated coal gasification combined cycle power plant in Buggenum, Netherlands. Appl Energy 2015;155:181–94.

[14] Kobayashi M, Akiho H, Nakao Y. Performance evaluation of porous sodium aluminate sorbent for halide removal process in oxy-fuel IGCC power generation plant. Energy 2015;92(3):320–7.

[15] Kobayashi M, Akiho H. Carbon behavior in the cyclic operation of dry desulfurization process for oxy-fuel integrated gasification combined cycle power generation. Energy Convers Manage 2016. http://dx.doi.org/10.1016/j.enconman.2016.03.02.

[16] Hashimoto T, Ota K, Fujii T. Progress update for commercial plants of air blown IGCC. In: Proceedings of ASME Turbo Expo, vol. 1; 2007. p. 499–504. http://dx.doi.org/10.1115/GT2007-28348.

[17] Ishibashi Y, Shinada O. First year operation results of CCP's Nakoso 250MW air-blown IGCC demonstration plant. Gasification technologies conference, Washington, DC, USA; 2008.

[18] Giuffrida A, Romano MC, Lozza G. Thermodynamic analysis of air-blown gasification for IGCC applications. Appl Energy 2011;88(11):3949–58.

[19] Giuffrida A, Romano MC, Lozza G. Efficiency enhancement in IGCC power plants with air-blown gasification and hot gas clean-up. Energy 2013;53:221–9.

[20] Mansouri Majoumerd M, De S, Assadi M, Breuhaus P. An EU initiative for future generation of IGCC power plants using hydrogen-rich syngas: simulation results for the baseline configuration. Appl Energy 2012;99:280–90.

[21] Cabezón PC, Llano PC, García-Peña F, Hervás N. CO_2 emissions reduction technologies in IGCC: ELCOGAS's experiences in the field. Greenhouse Gases: Sci Technol. 2013;3(4):253–65.

[22] Casero P, García Peña F, Coca P, Trujillo J. ELCOGAS 14 MWth pre-combustion carbon dioxide capture pilot. Technical and economical achievements. Fuel 2014;116:804–11.

[23] Urech J, Tock L, Harkin T, Hoadley A, Maréchal F. An assessment of different solvent-based capture technologies within an IGCC-CCS power plant. Energy 2014;64:268–76.

[24] Damen K, Faber R, Gnutek R, van Dijk HAJ, Trapp C, Valenz L. Performance and modelling of the pre-combustion capture pilot plant at the Buggenum IGCC. Energy Procedia 2014;63:6207–14.

[25] Trapp C, de Servi C, Casella F, Bardow A, Colonna P. Dynamic modelling and validation of pre-combustion CO_2 absorption based on a pilot plant at the Buggenum IGCC power station. Int J Greenhouse Gas Control 2015;36:13–26.

[26] Moioli S, Giuffrida A, Gamba S, Romano MC, Pellegrini L, Lozza G. Pre-combustion CO_2 capture by MDEA process in IGCC based on air-blown gasification. Energy Procedia 2014;63:2045–53.

[27] http://www.gecos.polimi.it/software/gs.php.

[28] Chiesa P, Macchi E. A thermodynamic analysis of different options to break 60% electric efficiency in combined cycle power plants. J Eng Gas Turbine Power 2004;126(4):770–85.

[29] Chiesa P, Lozza G, Mazzocchi L. Using hydrogen as gas turbine fuel. J Eng Gas Turbines Power 2005;127(1):73–80.

[30] Gazzani M, Chiesa P, Martelli E, Sigali S, Brunetti I. Using hydrogen as gas turbine fuel: premixed versus diffusive flame combustors. J Eng Gas Turbines Power 2014;136(5):051504.

[31] Giuffrida A, Romano MC. On the effects of syngas clean-up temperature in IGCCs. In: Proceedings of ASME Turbo Expo 2010; 2010 June 14–18; Glasgow, UK. http://dx.doi.org/10.1115/GT2010-22752.

[32] Giuffrida A, Romano MC, Lozza G. CO_2 capture from air-blown gasification-based combined cycles. In: Proceedings of ASME Turbo Expo 2012; 2012 June 11–15; Copenhagen, Denmark. http://dx.doi.org/10.1115/GT2012-69787.

[33] Giuffrida A. Impact of Low-Rank Coal on Air-Blown IGCC Performance. In: Proceedings of ASME Turbo Expo 2014; 2014 June 16–20; Düsseldorf, Germany. http://dx.doi.org/10.1115/GT2014-26843.

[34] Bonalumi D, Giuffrida A, Lozza G. A study of CO_2 capture in advanced IGCC systems by ammonia scrubbing. Energy Procedia 2014;45:663–70.

[35] Bonalumi D, Giuffrida A. Investigations of an air-blown IGCC fired with high-sulphur coal with post-combustion CCS by aqueous ammonia. Energy 2016. http://dx.doi.org/10.1016/j.energy.2016.04.025.

[36] Bonalumi D, Ciavatta A, Giuffrida A. Thermodynamic assessment of cooled and chilled ammonia-based CO_2 capture in air-blown IGCC plants. Energy Procedia 2016. http://dx.doi.org/10.1016/j.egypro.2016.01.028.

[37] Giuffrida A, Moioli S, Romano MC, Lozza G. Lignite-fired air-blown IGCC systems with pre-combustion CO_2 capture. Int J Energy Res 2016. http://dx.doi.org/10.1002/er.3488.

[38] EBTF. European best practice guidelines for assessment of CO_2 capture technologies; 2011.

[39] Chiesa P, Consonni S, Kreutz T, Williams R. Co-production of hydrogen, electricity and CO_2 from coal with commercially ready technology. Part A: Perform Emissions Int J Hydrogen Energy 2005;30:747–67.

[40] Korens N, Simbeck DR, Wilhelm DJ. Process screening analysis of alternative gas treating and sulfur removal for gasification. NETL-DOE report, Task order no. 739656-00100; 2002.

[41] Kohl AL, Nielsen R. Gas purification. 5th ed. Houston, Texas, USA: Gulf Publishing Company, Book Division; 1997.

[42] Chen CC, Britt HI, Boston JF, Evans LB. Extension and application of the Pitzer equation for vapor-liquid equilibrium of aqueous electrolyte systems with molecular solutes. AIChE J 1979;25:820–31.

[43] Chen CC, Britt HI, Boston JF, Evans LB. Local composition model for excess Gibbs energy of electrolyte systems. Part I: Single solvent, single completely dissociated electrolyte systems. AIChE J 1982;28:588–96.

[44] Mock B, Evans LB, Chen CC. Thermodynamic representation of phase equilibria of mixed-solvent electrolyte systems. AIChE J 1986;32:1655–64.

[45] Chen CC, Evans LB. A local composition model for the excess Gibbs energy of aqueous electrolyte systems. AIChE J 1986;32:444–54.

[46] Langé S, Pellegrini LA, Moioli S, Picutti B, Vergani P. Influence of gas impurities on thermodynamics of amine solutions. 2. Mercaptans. Ind Eng Chem Res 2013;52:2025–31.

[47] Pellegrini LA, Langé S, Moioli S, Picutti B, Vergani P. Influence of gas impurities on thermodynamics of amine solutions. 1. Aromatics. Ind Eng Chem Res 2013;52:2018–24.

[48] De Guido G, Langè S, Moioli S, Pellegrini LA. Thermodynamic method for the prediction of solid CO_2 formation from multicomponent mixtures. Process Saf Environ 2014;92:70–9.

[49] Langé S, Moioli S, Pellegrini LA. Vapor-liquid equilibrium and enthalpy of absorption of the CO_2-MEA-H_2O system. Chem Eng Trans 2015;43:1975–80.

[50] Renon H, Prausnitz JM. Local compositions in thermodynamic excess functions for liquid mixtures. AIChE J 1968;14:135–44.

[51] Moioli S, Pellegrini LA. Modeling the methyldiethanolamine-piperazine scrubbing system for CO_2 removal: thermodynamic analysis. Front Chem Sci Eng 2016;10:162–75.

[52] Astarita G, Savage DW, Bisio A. Gas treating with chemical solvents. New York: Wiley; 1983.

[53] Pinsent BRW, Pearson L, Roughton FWJ. The kinetics of combination of carbon dioxide with hydroxide ions. Trans Faraday Soc 1956;52:1512–8.

[54] Moioli S, Pellegrini LA, Picutti B, Vergani P. Improved rate-based modeling of H_2S and CO_2 removal by MDEA scrubbing. Ind Eng Chem Res 2013;52:2056–65.

[55] Moioli S, Pellegrini LA. Regeneration section of CO_2 capture plant by MEA scrubbing with a rate-based model. Chem Eng Trans 2013;32:1849–54.

[56] Zhang M, Guo Y. Rate based modeling of absorption and regeneration for CO_2 capture by aqueous ammonia solution. Appl Energy 2013;111:142–52.

[57] Lewis WK, Whitman WG. Principles of gas absorption. Ind Eng Chem 1924;16:1215–20.

[58] Fu K, Chen G, Liang Z, Sema T, Idem R, Tontiwachwuthikul P. Analysis of mass transfer performance of monoethanolamine-based CO_2 absorption in a packed column using artificial neural networks. Ind Eng Chem Res 2014;53:4413–23.

[59] Choi SY, Nam SC, Yoon YI, Park KT, Park S-J. Carbon dioxide absorption into aqueous blends of methyldiethanolamine (MDEA) and alkyl amines containing multiple amino groups. Ind Eng Chem Res 2014;53:14451–61.

[60] Park HM. Reduced-order modeling of carbon dioxide absorption and desorption with potassium carbonate promoted by piperazine. Int J Heat Mass Transf 2014;73:600–15.

[61] Cullinane JT. Thermodynamics and kinetics of aqueous piperazine with potassium carbonate for carbon dioxide absorption PhD thesis. Austin, Texas, USA: The University of Texas; 2005.

[62] Freguia S. Modeling of CO2 removal from flue gase with monoethanolamine M. S.E. thesis. Austin, Texas: The University of Texas; 2002.

[63] Chen X. Carbon dioxide thermodynamics, kinetics, and mass transfer in aqueous piperazine derivatives and other amines PhD thesis. Austin, Texas, USA: The University of Texas; 2011.

[64] Prasher BD, Fricke AL. Mass transfer at a free gas-liquid interface in turbulent thin films. Ind Eng Chem Proc Des Dev 1974;13:336–40.

[65] King CJ. Turbulent liquid phase mass transfer at a free gas-liquid interface. Ind Eng Chem Fundam 1966;5:1–8.

[66] Moioli S. The rate-based modelling of CO_2 removal from the flue gases of power plants. WIT Trans Ecol Environ 2014;186:635–46.

[67] Moioli S, Pellegrini LA. Improved rate-based modeling of the process of CO_2 capture with PZ solution. Chem Eng Res Des 2015;93:611–20.

[68] Moioli S, Pellegrini LA. Physical properties of PZ solution used as a solvent for CO_2 removal. Chem Eng Res Des 2015;93:720–6.

[69] Naami A, Edali M, Sema T, Idem R, Tontiwachwuthikul P. Mass transfer performance of CO_2 absorption into aqueous solutions of 4-diethylamino-2-butanol, monoethanolamine, and N-methyldiethanolamine. Ind Eng Chem Res 2012;51:6470–9.

[70] Daviet GR, Donnelly ST, Bullin JA. Dome's North Caroline plant successful conversion to MDEA. In: Sixty-third GPA annual convention. Tulsa: Gas Processor Association; 1984. p. 75–89.
[71] Walas SM. Chemical process equipment: selection and design. Stoneham, MA: Butterworths; 1988.
[72] Kidnay AJ, Parrish WR. Fundamentals of natural gas processing. Boca Raton, FL: Taylor & Francis Group; 2006.
[73] Rho S-W, Yoo K-P, Lee JS, Nam SC, Son JE, Min B-M. Solubility of CO_2 in aqueous methyldiethanolamine solutions. J Chem Eng Data 1997;42:1161–4.
[74] Lunsford KM, Bullin JA. Optimization of amine sweetening units. AIChE spring national meeting. New York: American Institute of Chemical Engineers; 1996.
[75] Polasek J, Bullin JA. Optimization of amine sweetening units GPA regional meeting. Tulsa, OK: Gas Processors Association; 1994.
[76] Guo XP, Tomoe Y. The effect of corrosion product layers on the anodic and cathodic reactions of carbon steel in CO_2-saturated mdea solutions at 100 °C. Corros Sci 1999;41:1391–402.
[77] Perry RH, Green DW. Perry's chemical engineers' handbook. 7th ed. Singapore: McGraw-Hill International Editions; 1997.
[78] NETL. Cost and performance baseline for fossil energy plants. Volume 1: bituminous coal and natural gas to electricity. report DOE/NETL-2010/1397, September 2013. <https://www.netl.doe.gov/File%20Library/Research/Energy%20Analysis/OE/BitBase_FinRep_Rev2a-3_20130919_1.pdf>.
[79] Cousins A, Wardhaugh LT, Feron PHM. A survey of process flow sheet modifications for energy efficient CO_2 capture from flue gases using chemical absorption. Int J Greenhouse Gas Control 2011;5:605–19.
[80] Neveux T, Le Moullec Y, Corriou JP, Favre E. Energy performance of CO_2 Capture processes: interaction between process design and solvent. Chem Eng Trans 2013;35:337–42.
[81] Spietz T, Wieclaw-Solny L, Tataczuk A, Krotki A, Stec M. Technological modifications in pilot research on CO_2 capture process. Chemick 2014;68:884–92.
[82] Shoeld M. Purifications and separation of gaseous mixtures. US patent no. 1971798; 1934.
[83] Towler GP, Shethna HK, Cole B, Hajdik B. Improved absorber-stripper technology for gas sweetening to ultra-low H2S concentrations. In: Proceedings of 76th GPA annual convention. Tulsa, OK.
[84] Cousins A, Wardhaugh LT, Feron PHM. Analysis of combined process flow sheet modifications for energy efficient CO_2 capture from flue gases using chemical absorption. Energy Procedia 2011;4:1331–8.
[85] Aroonwilas A, Veawab A. Heat recovery gas absorption process. Patent no. WO 2007/07004 A1; 2007.
[86] Meissner RE, Wagner U. Low-energy process recovers CO_2. Oil Gas J 1983;81 (5):55–8.
[87] Reddy S, Gilmartin J, Francuz V. Integrated compressor/stripper configurations and methods. Patent no. WO 2007075466 A2; 2007.